ISSN 1063-7796, Physics of Particles and Nuclei, 2010, Vol. 41, No. 4, pp. 543–573. © Pleiades Publishing, Ltd., 2010.
Original Russian Text © Yu.V. Popov, O. Chuluunbaatar, V.L. Shablov, K.A. Kouzakov, 2010, published in Fizika Elementarnykh Chastits i Atomnogo Yadra, 2010, Vol. 41, No. 4.

Multiple Ionization Processes Involving Fast Charged Particles

Yu. V. Popov[a], O. Chuluunbaatar[b], V. L. Shablov[c], and K. A. Kouzakov[d]

[a] *Institute of Nuclear Physics, Moscow State University, Moscow, 119991 Russia*
[b] *Joint Institute for Nuclear Research, Dubna, Moscow region, 141980 Russia*
[c] *Obninsk State Technical University for Nuclear Power Engineering, Obninsk, Kaluga region, 249040 Russia*
[d] *Faculty of Physics, Moscow State University, Moscow, 119991 Russia*
e-mail: popov@srd.sinp.msu.ru, chuka@jinr.ru

Abstract—This review is devoted to certain aspects of the theory of multiple ionization of a quantum target by a fast charged particle. Atoms and molecules, and their ions as well, are considered as targets, while electrons and protons are considered as projectiles. Special attention is paid to the effective charge approximation while constructing continuum wave functions for several charged fragments in the exit channel of the reaction. Theoretical calculations of differential and total cross sections of various multiple ionization processes are presented and, where possible, comparison of the results of these calculations with experimental data is carried out.

DOI: 10.1134/S1063779610040040

CONTENTS

INTRODUCTION

Theoretical analysis of multiple ionization of an atomic or molecular target by the impact of a fast moving particle (an electron, proton, ion, photon, a group of photons) is a daunting task in nonrelativistic physics. Although it is sometimes manageable to describe a fast particle by the plane wave and thereby reduce the problem to the Born approximations in the interaction with a neutral atom (a molecule), it is not much help either. The appearance of a few, often slowly moving, electrons at the end of the reaction requires an application of the scattering theory of few charged particles. In the case of three neutral particles, such a theory was formulated and mathematically justified [1, 2]. In the case of three charged particles, the boundary conditions for the differential problem of calculating a wave function in the configuration space have been formulated in a mathematically correct way [2, 3]. Certain approaches to formulating the scattering problem of three charged particles in the momentum space for scattering amplitudes can be found in the references cited in a recent review [4]. In particular, there are discussions concerning the extra singularities of scatter-

ing amplitudes of a few Coulomb particles and the ways to eliminate them when the collision energy becomes on-shell, i.e., there appears a link between the energy and momentum of particles.

The mentioned singularities appear in higher orders of perturbation theory when there is the Green's function of free wave equation in the matrix element of scattering amplitude. The first order (FBA) is usually free of these issues. However, what is FBA anyway? The Hamiltonian pertaining to the problem must be divided into a sum of at least two terms $H = H_0 + V$, where H_0 is a free Hamiltonian and V denotes an interaction. Then FBA is written in the form of the matrix element

$$T_{fi} = \langle \Psi_f^- | V | \Psi_i^+ \rangle, \qquad \text{(I.1)}$$

where the initial $|\Psi_i^+\rangle$ and final $|\Psi_f^-\rangle$ wave functions of a system belong to the spectrum of the Hamiltonian H_0. Such processes are called direct. In the processes with rearrangement, the full Hamiltonian H is represented in a twofold way, $H = H_{0i} + V_i = H_{0f} + V_f$ thereby leading to the formula

$$T_{fi} = \langle \Psi_f^- | V_i | \Psi_i^+ \rangle = \langle \Psi_f^- | V_f | \Psi_i^+ \rangle. \qquad \text{(I.2)}$$

Expressions (I.1) and (I.2) are exact in FBA, but the functions $|\Psi_f^-\rangle$ and $|\Psi_i^+\rangle$ are solutions to the multiparticle differential (integral) equations that can often be hardly solved even numerically, since it is impossible to formulate boundary conditions adequate to the problem at hand.

Here we set foot on a shaky ground of approximations.

The main idea of most of those approximations is separability of the final multielectron function. Roughly speaking, the part of an eigenfunction being a product of functions is extracted in the Schrödinger equation for the wave function $|\Psi_f^-\rangle$, while the remaining one is taken to be a perturbation and is omitted in FBA. Often, such an approach is based on asymptotic considerations. However, to do so is far from easy if we intend to describe a maximally possible number of phenomena in FBA. The obstacles to this are the potentials of electron–electron interaction leading to diverse effects of electron correlations. It is quite problematic to somehow "approximate" them in a sensible way. This is why in Section 1 we consider mathematical foundations of the effective charge method formulated taking into account higher order perturbative divergences, which were extensively discussed in our previous review [4].

Here we are mainly concerned with those multiple ionization reactions in which an atomic target emits no less than two electrons upon interaction with a fast particle (the simplest cases are a helium atom and hydrogen molecule). Of course, it is unfortunate to have to set aside the nearly limitless and still developing theoretical and experimental aspects of single ionization reactions that have been determined so far. However, with complex targets, we will not be able to avoid completely the consideration of (e,2e) reactions, as the final states of (e,2e) and (e,3e) reactions on the same target are in fact different eigenfunctions of its Hamiltonian and comparisons are inevitable. And only in the last, fourth, section we will consider (e,2e) reactions on molecular targets. This in no way is new material, but it should be mentioned that even the simplest hydrogen molecule is a system of four bodies, and recently we have witnessed a number of interesting approximate approaches and numerical methods that will be presented and discussed here.

The direct processes of multiple ionization differ in the number of electrons in the final state. It is supposed that the final fast particles are measured in coincidence between each other and with slow moving emitted electrons as well. If, for definiteness, one talks of multielectron target ionization by fast electrons (with energies of a few keV), then there are the so-called dipole (e,3e) reactions, in which an incoming electron transfers a small amount of the momentum and energy to an atom and, therefore, goes out with almost unchanged velocity, and quasi-elastic (e,3e) reactions (or electron momentum spectroscopy (EMS)), when there are two fast electrons in the final state with nearly identical energies and angles. The differential cross sections of (e,3e) processes with completely measured angles and energies of all three final electrons are extremely small [5, 6], especially in the case of EMS [7]. Therefore, one resorts to the measurements of cross sections of lower multiplicity, say, (e,3—1e), when no slowly moving electron is detected [8]. Although (e,3e) experiments in quasi-elastic kinematics are rare nowadays, they are quite informative in effectively discerning a degree of electron pair correlations in the multiparticle wave function of a target [7, 8].

Transfer ionization (TI) by a fast incoming proton (with the energy of several MeV) can be considered a multiple ionization reaction. In the course of the impact, the target loses at least two electrons, one of which is captured by a proton, thus creating a fast moving hydrogen atom. Here the diverse final states of the fragments and their combinations are possible: the ground (excited) state of a hydrogen atom, ground (excited) state of an ion-residue, molecule ion dissociation (in the case of a molecular target), etc. A measurement in coincidence of various reaction products may give exclusive information on the mechanisms of the reaction studied. At the moment, rather extensive experimental data are obtained.

Section 2 will be devoted to reactions with two fast particles produced in the final state.

In so-called dipolar experiments, there is a single fast particle in the final state, the one that bombarded the target. Such experiments provide a higher coincidence event rate and, therefore, are more popular among experimenters. At the same time, this requires

theorists to construct a three-body final state function of two "free" electrons in the field of an ion, or even its adequate approximation. We will consider these issues in a bit more detail in Section 3.

It is not the purpose of this review to present every single approximation in the theory existing to date. As is known, "no living man all things can." At times, scientists try to match their theoretical models with the experiment by somehow "adjusting" a classical approximate scheme. Then, numerous abbreviations appear on the market, announcing the introduction of another parameter in known approximations that are sometimes limited by the paper the model is presented in. It is virtually impossible to sort that mess out. Moreover, today, theorists calculate matrix elements numerically and, thereby, often make understanding of the physics of the processes that take place more difficult. It is not always obvious what is coded in the programs, what the real accuracy of the results is, and what we have as an output.

It is widely believed that the study of multiple ionization processes enables a much deeper understanding of the role of electron correlations in the target and lets one go beyond the Hartree–Fock single-particle models. This is indeed the case, but this general statement is not always based on clear-cut physics. That is why we, first, consider prompt processes that allow only the first Born approximation with transparent reaction mechanisms to be used in most cases. Second, fast particles enable the complex multiparticle Coulomb function of freely moving reaction fragments to be further reduced based on physically justified simplifications. Third, numerical calculations of the matrix elements are limited to multiple integration, which is, though being complicated, a much better developed calculation method than, say, the integration of multidimensional differential (integral) equations in the multiparticle scattering theory.

In concluding this introductory discussion, we would like to cite a number of review articles and books related to the problem considered here that include a large number of references to the original works. First of all, this concerns the classic work by Peterkop [10] dedicated to the theory of electron impact ionization of atoms that includes references to books and basic original works up to 1970, in particular, books by Drukarev, Mott and Messi, Wu and Omura, Rudge and Seaton, etc, where even earlier approximations and methods that became classical were reviewed. The experimenter's point of view on the problem of electron impact ionization is given in [12], which is replete with references to original works up to 1990. Of more recent reviews, we should mention [13].

Besides those cited above, there are a number of reviews devoted to the specific topic of electron momentum spectroscopy that have been published in the literature. These are book by Weigold and McCarthy [14] and review by Coplan et al. [15], in addition to review by Neudachin et al. [7] mentioned earlier. However, in most of these works, the case of (e,2e) reactions is considered, with a huge experimental database related to the latter and collected during the 1960s to 1980s.

It is worth mentioning excellent review by Briggs and Schmidt [16] dedicated to (γ,2e) reactions, as well as that by Sadeghpour [17] with references to works up to 1995. At last, the reader can familiarize himself with the issues of "two-electronic" atoms' behavior in strong electric field, including the case in which the latter varies with time, by referring to [18]. This last problem has been rapidly developing of late and deserves a separate review in the journal *Fizika elementarnykh chastits i atomnogo yadra* (Physics of Particles and Nuclei). We are not going to touch on it here, since the theory of such reactions is based on the time-dependent Schrödinger equation and requires other theoretical schemes and approximations to be employed.

The literature related with the problem of capture is more extensive, which is expected considering the practical importance of this topic. A detailed account of the theory of ion–atom collisions is given in book [19] and reviews [20] and [21], whereas a considerable amount of the experimental data on inelastic collisions of fast charged particles with atoms and molecules and its comparison with the Bethe theory are presented in classic review by Inokuti [22].

If not otherwise defined, the atomic units $e = m_e = \hbar = 1$ are used throughout. Additionally, the plane (azimuthal) angles of particle momentum vectors are counted from the direction of incoming particle's velocity vector counterclockwise in most of the illustrating figures borrowed from various sources. Otherwise, it is defined in the corresponding figure caption.

1. EFFECTIVE CHARGE METHOD IN THE PROBLEM OF TWO ELECTRONS IN THE FIELD OF A NUCLEUS AT REST

The best known method of factorizing the continuum function of three charged particles is the method of effective charges, which is a variation of the distorted wave method. It was developed by Peterkop [9, 10] and Rudge and Seaton [11] and based on classical motion dynamics of two electrons in the field of nucleus at large relative distances between all three components of the system. Indeed, according to the correspondence principle in quantum mechanics, asymptotic motion of electrons from the collision region toward detectors is defined by the classical relations $\mathbf{r}_i = \mathbf{k}_i|t|$. In this case, the interaction potential can be written in the form

$$-\frac{Z}{r_1}-\frac{Z}{r_2}+\frac{1}{r_{12}} = \frac{1}{|t|}\left(-\frac{Z}{k_1}-\frac{Z}{k_2}+\frac{1}{2k_{12}}\right), \qquad (1.1)$$

where $r_{12} = |\mathbf{r}_1 - \mathbf{r}_2|^{-1}$, $2k_{12} = |\mathbf{k}_1 - \mathbf{k}_2|^{-1}$, and Z is the charge of a nucleus. The right-hand side of Eq. (1.1) can now be rewritten to take the following form:

$$\frac{1}{|t|}\left(-\frac{Z}{k_1}-\frac{Z}{k_2}+\frac{1}{2k_{12}}\right)=\frac{1}{|t|}\left(-\frac{Z_1}{k_1}-\frac{Z_2}{k_2}\right)=\left(-\frac{Z_1}{r_1}-\frac{Z_2}{r_2}\right), \tag{1.2}$$

introducing effective charges Z_1 and Z_2. From this we obtain the equation for these two charges,

$$\frac{Z}{k_1}+\frac{Z}{k_2}-\frac{1}{2k_{12}}=\frac{Z_1}{k_1}+\frac{Z_2}{k_2}, \tag{1.3}$$

and the finite nonsymmetrized wave function represented by a product of two Coulomb functions,

$$\Psi^{-*}(\mathbf{k}_1,\mathbf{k}_2;\mathbf{r}_1,\mathbf{r}_2)\approx\varphi^{-*}(\mathbf{k}_1,\mathbf{r}_1;Z_1)\times\varphi^{-*}(\mathbf{k}_2,\mathbf{r}_2;Z_2). \tag{1.4}$$

In Eq. (1.4) the Coulomb function is chosen to be

$$\varphi^{-*}(\mathbf{p},\mathbf{r};Z_{eff})=e^{-\pi\xi/2}\Gamma(1+i\xi)\times e^{-i\mathbf{pr}}{}_1F_1(-i\xi,1;ipr+i\mathbf{pr});\quad \xi=-\frac{Z_{eff}}{p}. \tag{1.5}$$

Despite the elegance of formula (1.4), the product of two Coulomb functions cannot be used as a free term of a Lippmann–Schwinger (LS) equation with a compact kernel, since the perturbative potential

$$V_{\text{pert}}=-\frac{Z-Z_1}{r_1}-\frac{Z-Z_2}{r_2}+\frac{1}{r_{12}}$$

does not cease to be long-range. Moreover, this potential is also nonlocal, as it depends on the energies of electrons. However, the problem can be solved. We shall consider the effective charge method within the framework of the consistent theory given in some detail in [4] (see Subsection 1.4 for the distorted wave method). Here we will just briefly recall the main results necessary for the presentation of new material.

1.1. Integral Equations of the Few-Particle Scattering Theory with Coulomb Interaction

For generality, let us introduce the notion of the reaction channel α and denote by $\mathbf{p}_\alpha$ a set of relative Jacobi momenta $\mathbf{p}_{\beta\gamma}$ that define the motion of N_α fragments colliding in the channel α. The relative coordinate of particles i and j is $\mathbf{r}_{ij}$, while their relative momentum is denoted as $\mathbf{k}_{ij}$. The wave vector $|\phi_\alpha\rangle$ is a product of the wave vectors of bound states of the fragments defining the channel α, with the total binding energy $-\kappa_\alpha^2$. In this way, the asymptotic wave vector of the channel α takes the form $|\phi_\alpha, \mathbf{p}_\alpha\rangle$. V^α denotes the sum of pair interaction potentials between particles belonging to different fragments that collide in the channel α. Let us define also the Coulomb parameter (the Coulomb number or Sommerfeld parameter) of the channel α,

$$\eta_\alpha=\sum_{\beta,\gamma}\eta_{\beta\gamma}=\sum_{\beta,\gamma}\frac{q_\beta q_\gamma\mu_{\beta\gamma}}{p_{\beta\gamma}},$$

which is equal to the sum of the Coulomb parameters of a pair of fragments β and γ, $\mu_{\beta\gamma}$ is the reduced mass of these fragments, q_β and q_γ are their total charges. Finally, we define the Dollard phase of α channel [23]:

$$A_\alpha=\sum_{\beta,\gamma}\eta_{\beta\gamma}\ln\frac{2p_{\beta\gamma}^2}{\mu_{\beta\gamma}}=\sum_{\beta,\gamma}\eta_{\beta\gamma}\ln 4E_{\beta\gamma},$$

where $E_{\beta\gamma}$ is the energy of relative motion of β and γ fragments. The channel of complete dissociation (without any bound states) is denoted by the index "0".

Consider for simplicity the reaction of dissociation of a two-body neutral bound pair by an incoming charged particle (not necessarily fast). The interaction potential of such a system can be written in the following form:

$$V=\sum_{i<j}\frac{q_iq_j}{r_{ij}}=\sum_{\gamma=1}^{3}\frac{\lambda_\gamma}{r_\gamma}. \tag{1.6}$$

Now define the operator

$$T(z)=V^\alpha+VG(z)V^\alpha, \tag{1.7}$$

where $G(z)=(z-H_0-V)^{-1}$ and H_0 is the free Hamiltonian of three particles. The operator in (1.7) specifies the dissociation amplitude of a neutral pair α (e.g., an atom) and satisfies the integral LS equation

$$T(z)=V^\alpha+VG_0(z)T(z). \tag{1.8}$$

In this equation, the operator $G_0(z)=(z-H_0)^{-1}$ stands for the free Green's function.

Following [2, 24, 25] (see also general definition (1.27) in [4]) the operator $T(z)$ can be written in the form

$$T(z)=(z-H_0)^{i\hat{\eta}}M(z)+R(z). \tag{1.9}$$

The matrix elements $\langle\mathbf{k}_\gamma,\ \mathbf{p}_\gamma|M(z)|\mathbf{p}_\alpha^0,\ \phi_\alpha\rangle$ and $\langle\mathbf{k}_\gamma,\mathbf{p}_\gamma|R(z)|\mathbf{p}_\alpha^0,\ \phi_\alpha\rangle$ are nonsingular in the transition $z\longrightarrow E+i0=k_\gamma^2/(2\mu_\gamma)+p_\gamma^2/(2\eta_\gamma)+i0$. A pair of Jacobi momenta $(\mathbf{k}_\gamma, \mathbf{p}_\gamma)$ correspond to the exit dissociation channel, where three such equivalent sets can be defined, and $\mathbf{p}_\alpha^0$ is the momentum of an incoming particle (an electron) with respect to a bound pair in the entrance channel α.

If the operator $M(z)$ is known, then the desired nonsingular reaction amplitude can be defined on the energy shell as follows [2, 24, 25]:

$$t(\mathbf{k}_\gamma, \mathbf{p}_\gamma, \mathbf{p}_\alpha^0) = \frac{\exp\left(-\frac{\pi}{2}\eta + iA_0\right)}{\Gamma(1-i\eta)} \times \langle \mathbf{k}_\gamma, \boldsymbol{p}_\alpha | M(E+i0) | \mathbf{p}_\alpha^0, \phi_\alpha \rangle. \quad (1.10)$$

Unfortunately, it turns out that no equation with a compact kernel can be formulated for the operator $M(z)$; therefore, the only way is to explicitly resolve a singularity out of the solution to the LS equation, which in certain cases leads to regularizations (renormalizations). This topic is covered in [4].

At the same time, the operator $R(z)$ in (1.9) does not possess any physical meaning and its matrix element vanishes while going to the energy shell [2, 25]. This helpful observation is used in formulating the effective charge method.

For the final state with given momenta $\mathbf{k}_\gamma$ and $\mathbf{p}_\gamma$, we define the nonlocal (energy dependent) pair potential $U = \lambda_\gamma / r_\gamma$ with effective charge $\lambda_\gamma = \eta k_\gamma / \mu_\gamma$ and transform Eq. (1.8) in the following manner:

$$T(z) = [I - UG_0(z)]^{-1} V^\alpha + [I - UG_0(z)]^{-1}(V-U)G_0(z)T(z).$$

It is possible to write the equality

$$[I - UG_0(z)]^{-1} = I + t_U(z)G_0(z),$$

where the operator $t_U(z)$ corresponds to the scattering amplitude on the potential U. As a result, we obtain

$$T(z) = [I + t_U(z)G_0(z)]V^\alpha + [I + t_U(z)G_0(z)](V-U)G_0(z)T(z). \quad (1.11)$$

The purpose of introducing the potential U is to compensate a three-body singularity $(z-E)^{i\eta}$ in the matrix element $\langle \mathbf{k}_\gamma, \mathbf{p}_\gamma | (V-U)G_0(z)T(z) | \mathbf{p}_\alpha^0, \phi_\alpha \rangle$ in the limit $z \longrightarrow E + i0$ by introducing an additional two-body Coulomb singularity (see also formula (1.47) in [4]). Therefore, the two-body potential must necessarily be dependent on the energy.

1.2. Second Born Approximation for the Breakup Amplitude

Taking into account relations (1.10) and (1.11), the following expression for the physical scattering amplitude can be written:

$$t(\mathbf{k}_\gamma, \mathbf{p}_\gamma, \mathbf{p}_\alpha^0) = \exp\left(-i\eta \ln\frac{2k_\gamma^2}{\mu_\gamma} + iA_0\right) \times [\langle \varphi_\gamma^-(\mathbf{k}_\gamma), \mathbf{p}_\gamma | V^\alpha | \mathbf{p}_\alpha^0, \phi_\alpha \rangle + \langle \varphi_\gamma^-(\mathbf{k}_\gamma), \mathbf{p}_\gamma | (V-U)G_0(E+i0)T(E+i0) | \mathbf{p}_\alpha^0, \phi_\alpha \rangle], \quad (1.12)$$

where $\varphi_\gamma^-(\mathbf{k}_\gamma)$ is the two-body Coulomb function corresponding to the potential U. After simple transformations, Eq. (1.12) can be rewritten to take the well-known form

$$t(\mathbf{k}_\gamma, \mathbf{p}_\gamma, \mathbf{p}_\alpha^0) = \exp\left(-i\eta \ln\frac{2k_\gamma^2}{\mu_\gamma} + iA_0\right) \times \langle \varphi_\gamma^-(\mathbf{k}_\gamma), \mathbf{p}_\gamma | (V-U) | \Psi_\alpha^+(\mathbf{p}_\alpha^0) \rangle, \quad (1.13)$$

which was for the first time obtained by Peterkop [10]. FBA in the effective charge method is given by the expression

$$t_1(\mathbf{k}_\gamma, \mathbf{p}_\gamma, \mathbf{p}_\alpha^0) = \exp\left(-i\eta \ln\frac{2k_\gamma^2}{\mu_\gamma} + iA_0\right) \times \langle \varphi_\gamma^-(\mathbf{k}_\gamma), \mathbf{p}_\gamma | (V-U) | \phi_\alpha, \mathbf{p}_\alpha^0 \rangle. \quad (1.14)$$

Before SBA is defined, consider the sum

$$\sum_\gamma \exp\left(i\eta \ln\frac{2k_\gamma^2}{\mu_\gamma}\right)\frac{\eta_\gamma}{\eta} t(\mathbf{k}_\gamma, \mathbf{p}_\gamma, \mathbf{p}_\alpha^0), \quad (1.15)$$

with the amplitude $t(\mathbf{k}_\gamma, \mathbf{p}_\gamma, \mathbf{p}_\alpha^0)$ presented in (1.13). In order to compute the sum in Eq. (1.15), we mark the potential U by the index γ, which was so far omitted to simplify the notation, and take into account the following chain of equalities:

$$\sum_\gamma \frac{\eta_\gamma}{\eta}(V - U_\gamma) = V - \sum_\gamma \frac{\eta_\gamma k_\gamma}{\mu_\gamma r_\gamma} = V - \sum_\gamma \frac{\lambda_\gamma}{r_\gamma} = 0.$$

In addition, we write, without proof, the expression for the convolution of Coulomb function with smooth function $f(\mathbf{k})$:

$$\langle \varphi^-(\mathbf{k}) | f \rangle = \exp\left(-\frac{\pi}{2}\eta\right)\Gamma(1+i\eta)f(\mathbf{k}) + \int d\mathbf{k}' \langle \varphi^-(\mathbf{k}) | V_c (E - h_0 + i0)^{-1} | \mathbf{k}' \rangle (f(\mathbf{k}') - f(\mathbf{k})) = \exp\left(-\frac{\pi}{2}\eta\right)\Gamma(1+i\eta)f(\mathbf{k}) + \int d\mathbf{k}' \langle \mathbf{k} | V_c (E - h_0 + i0)^{-1} | \mathbf{k}' \rangle (f(\mathbf{k}') - f(\mathbf{k})) + (\text{higher order terms}). \quad (1.16)$$

All these auxiliary calculations let Eq. (1.13) be represented in the form

$$t(\mathbf{k}_\gamma, \mathbf{p}_\gamma, \mathbf{p}_\alpha^0) = N \sum_\gamma \frac{\eta_\gamma}{\eta} \times (\langle \varphi^-(\mathbf{k}_\gamma), \mathbf{p}_\gamma | V^\alpha | \phi_\alpha, \mathbf{p}_\alpha^0 \rangle + Y(\mathbf{k}_\gamma, \mathbf{p}_\gamma; \mathbf{p}_\alpha^0; E+i0)). \quad (1.17)$$

The factor N in (1.17) is equal to

$$e^{iA_0}\left(\sum_\gamma \frac{\eta_\gamma}{\eta} \exp\left(i\eta \ln\frac{2k_\gamma^2}{\mu_\gamma}\right)\right)^{-1},$$

and the function Y can be written as

$$Y(\mathbf{k}_\gamma, \mathbf{p}_\gamma; \mathbf{p}_\alpha^0; E+i0) = \sum_\gamma \int d\mathbf{k}_\gamma' \left(\frac{k_\gamma^2}{2\mu_\gamma} - \frac{k_\gamma'^2}{2\mu_\gamma} + i0\right)^{-1} \times \langle \psi_\gamma^-(\mathbf{k}_\gamma)|U_\gamma|\mathbf{k}_\gamma'\rangle \times [\langle \mathbf{k}_\gamma', \mathbf{p}_\gamma|(V-U_\gamma)G_0(E+i0)T(E+i0)|\mathbf{p}_\alpha^0, \phi_\alpha\rangle - \langle \mathbf{k}_\gamma, \mathbf{p}_\gamma|(V-U_\gamma)G_0(E+i0)T(E+i0)|\mathbf{p}_\alpha^0, \phi_\alpha\rangle], \quad (1.18)$$

and clearly includes the Born terms in potentials higher than the second one. It can be omitted in SBA, with the remaining part in (1.17) corresponding to the second order approximation. It turns out that, in the second Born approximation the effective charges in (1.13) can be fixed; this is considered in the next subsection.

1.3. Two Particles in the Coulomb Field of a Fixed Center

For convenience, let us somewhat alter the variable notations. Consider the process $(23) + 1 \longrightarrow 1 + 2 + 3$, where an infinitely heavy nucleus (a center) is denoted by the index (3), $|\phi_2\rangle$ stands for the wave function of the initial bound state, and $\mathbf{k}_0$ is the momentum of the incoming particle, while $\mathbf{k}_1$ and $\mathbf{k}_2$ are those of the final particles. These latter particles may well be electrons.

Equation (1.11) in the new notation looks like

$$T(z) = [I + t_{1,2}(z)G_0(z)](V-U_{1,2}) + [I + t_{1,2}(z)G_0(z)](V-U_{1,2})G_0(z)T(z). \quad (1.19)$$

The operator $t_{1,2}(z)$ denotes the scattering amplitude on the potential $U_{1,2} = U_1 + U_2$, where $U_j = -Z_j q_j/r_j$ ($j = 1, 2$) and the constants Z_j are the effective charges, while, in the general case (see (1.3)),

$$-\frac{Z_1 q_1}{v_1} - \frac{Z_2 q_2}{v_2} = \tilde{\eta}_1 + \tilde{\eta}_2 = \eta = \eta_1 + \eta_2 + \eta_{12} = -\frac{Zq_1}{v_1} - \frac{Zq_2}{v_2} + \frac{q_1 q_2}{v_{12}}. \quad (1.20)$$

Here $\mathbf{v}_j = \mathbf{k}_j/m_j$ is the velocity of a light particle, q_j is its charge, and $\mathbf{v}_{12} = \mathbf{v}_1 - \mathbf{v}_2$ denotes the relative velocity of light particles.

From (1.12) it follows that

$$t(\mathbf{k}_1, \mathbf{k}_2, \mathbf{k}_0) = \exp(-i(A_0 - \tilde{A}_{1,2})) \times [\langle \varphi_1^-(\mathbf{k}_1), \varphi_2^-(\mathbf{k}_2)|(V-U_{1,2})|\mathbf{k}_0, \phi_2\rangle + \langle \varphi_1^-(\mathbf{k}_1), \varphi_2^-(\mathbf{k}_2)|(V-U_{1,2}) \times G_0(E+i0)T(E+i0)|\mathbf{k}_0, \phi_2\rangle], \quad (1.21)$$

where $|\varphi_i^-(\mathbf{k}_i)\rangle$ is the Coulomb wave function describing the scattering on the potential U_i, and

$$A_0 = \eta_1 \ln 4E_1 + \eta_2 \ln 4E_2 + \eta_{12} \ln 4E_{12},$$
$$\tilde{A}_{1,2} = \tilde{\eta}_1 \ln 4E_1 + \tilde{\eta}_2 \ln 4E_2.$$

However, it is possible to choose another potential U and, correspondingly, another expression for Eq. (1.12)

$$t(\mathbf{k}_1, \mathbf{k}_2, \mathbf{k}_0) = \exp(-i(A_0 - \tilde{A}_{12})) \times [\langle \varphi_{12}^-(\mathbf{k}_{12}), \mathbf{K}_{12}|(V-U_{12})|\mathbf{k}_0, \phi_2\rangle + \langle \varphi_{12}^-(\mathbf{k}_{12}), \mathbf{K}_{12}|(V-U_{12})G_0(E+i0)T(E+i0)|\mathbf{k}_0, \phi_2\rangle], \quad (1.22)$$

where

$$U_{12} = \frac{\eta k_{12}}{\mu_{12}}\frac{1}{r_{12}} = \frac{\lambda_{12}}{r_{12}}, \quad \tilde{A}_{12} = \tilde{\eta}_{12} \ln 4E_{12},$$

and $\mathbf{k}_{12} = (m_2\mathbf{k}_1 - m_1\mathbf{k}_2)/(m_1 + m_2)$ and $\mathbf{K}_{12} = \mathbf{k}_1 + \mathbf{k}_2$ are the relative momentum in a pair (12) and its total momentum, respectively.

Now we apply the scheme given in (1.16) to (1.21) and (1.22). As a result, we obtain

$$\exp(i(A_0 - \tilde{A}_{1,2}))t(\mathbf{k}_1, \mathbf{k}_2, \mathbf{k}_0) = \langle \varphi_1^-(\mathbf{k}_1), \varphi_2^-(\mathbf{k}_2)|(V-U_{1,2})|\mathbf{k}_0, \phi_2\rangle + \exp\left(-\frac{\pi}{2}\eta\right)\Gamma(1+i\tilde{\eta}_1)\Gamma(1+i\tilde{\eta}_2) \times \langle \mathbf{k}_1, \mathbf{k}_2|(V-U_{1,2})G_0(E+i0)T(E+i0)|\mathbf{k}_0, \phi_2\rangle + (\text{higher order terms}) \quad (1.23.1)$$

and

$$\exp(i(A_0 - \tilde{A}_{12}))t(\mathbf{k}_1, \mathbf{k}_2, \mathbf{k}_0) = \langle \varphi_{12}^-(\mathbf{k}_1), \mathbf{K}_{12}|(V-U_{12})|\mathbf{k}_0, \phi_2\rangle + \exp\left(-\frac{\pi}{2}\eta\right)\Gamma(1+i\eta) \times \langle \mathbf{k}_{12}, \mathbf{K}_{12}|(V-U_{12})G_0(E+i0)T(E+i0)|\mathbf{k}_0, \phi_2\rangle + (\text{higher order terms}). \quad (1.23.2)$$

Next, construct a linear combination of expressions (1.23), namely,

$$\exp(iA_0)\left(\frac{x\exp(-i\tilde{A}_{1,2})}{\Gamma(1+i\tilde{\eta}_1)\Gamma(1+i\tilde{\eta}_2)} + \frac{y\exp(-i\tilde{A}_{12})}{\Gamma(1+i\eta)}\right) \times t(\mathbf{k}_1, \mathbf{k}_2, \mathbf{k}_0) = \frac{x\langle \varphi_1^-(\mathbf{k}_1), \varphi_2^-(\mathbf{k}_2)|(V-U_{1,2})|\mathbf{k}_0, \phi_2\rangle}{\Gamma(1+i\tilde{\eta}_1)\Gamma(1+i\tilde{\eta}_2)} + \frac{y}{\Gamma(1+i\eta)}\langle \varphi_{12}^-(\mathbf{k}_{12})\mathbf{K}_{12}|(V-U_{12})|\mathbf{k}_0, \phi_2\rangle + \exp\left(-\frac{\pi}{2}\eta\right)\langle \mathbf{k}_1, \mathbf{k}_2|((x+y)V - xU_{1,2} - yU_{12}) \times G_0(E+i0)T(E+i0)|\mathbf{k}_0, \phi_2\rangle, \quad (1.24)$$

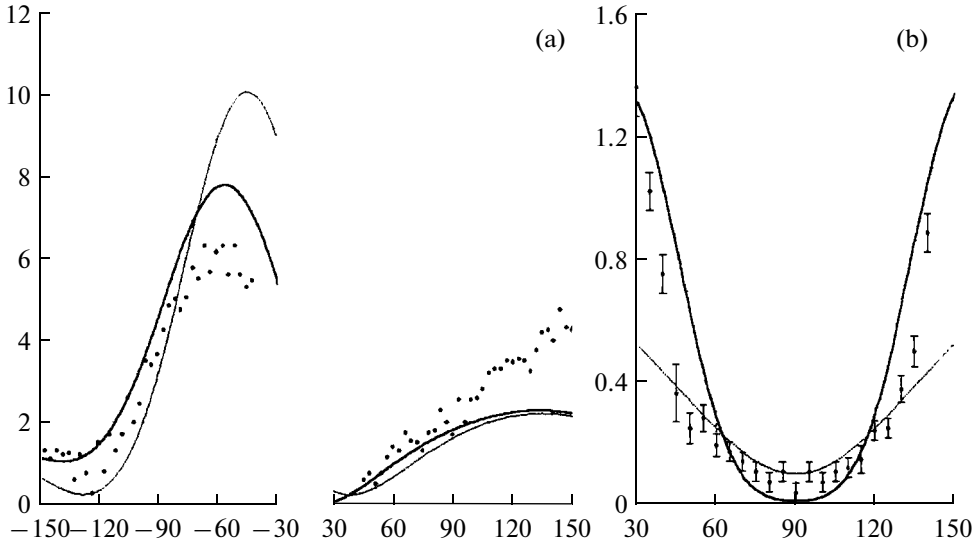

Fig. 1. TDCS (Y axis) for the reaction H(e,2e)H^+: (a)—asymmetric plane geometry, $E_0 = 150$ eV, $E_2 = 5$ eV, $\theta_1 = 4°$, X axis stands for the slow electron scattering angle θ_2, measured counterclockwise with a plus sign and clockwise with a minus sign from the incoming electron direction; (b)—symmetric plane geometry, $E_1 = E_2 = 2$ eV, $\theta_1 = \theta_2 + \pi$ (X axis). Experimental points are from [27, 28]. The figure is borrowed from [26].

with still arbitrary constants x and y. Now assume

$$(x+y)V - xU_{1,2} - yU_{12} = 0, \tag{1.25}$$

which leads to disappearance of the last term in (1.24).

If the charge of a Coulomb center is denoted via Z, then the potential V is in general written in the form

$$V = -\frac{Zq_1}{r_1} - \frac{Zq_2}{r_2} + \frac{q_1q_2}{r_{12}}.$$

From (1.25) the system of algebraic equations

$$\begin{cases} -(x+y)Z + Z_1x = 0, \\ -(x+y)Z + Z_2x = 0, \\ (x+y)q_1q_2 - \lambda_{12}y = 0. \end{cases} \tag{1.26}$$

follows, which immediately leads to the equality of effective charges $Z_1 = Z_2$. Now, setting $y = x\xi$, taking into account(1.20), the solutions we are interested in are obtained from (1.26)

$$Z_1 = Z_2 = \frac{(Zq_1v_2v_{12} + Zq_2v_1v_{12} - q_1q_2v_1v_2)}{v_{12}(q_1v_2 + q_2v_1)},$$

$$\lambda_{12} = \frac{Z_jq_1q_2}{Z_j - Z}, \quad \xi = \frac{Z_j - Z}{Z}.$$

Substituting this in (1.24), we derive the final SBA expression for the amplitude within a framework of the effective charge method:

$$\begin{aligned} &\exp(-iA_0)(\Gamma(1+i\eta)\exp(-i\tilde{A}_{1,2}) \\ &+ \xi\exp(-i\tilde{A}_{12})\Gamma(1+i\tilde{\eta}_1)\Gamma(1+i\tilde{\eta}_2))^{-1} \\ &\times [\Gamma(1+i\eta)\langle\varphi_1^-(\mathbf{k}_1), \varphi_2^-(\mathbf{k}_2) \\ &\times \left|\left(V + \frac{Z_{1q1}}{r_1} + \frac{Z_{2q2}}{r_2}\right)\right|\mathbf{k}_0, \phi_2\rangle + \Gamma(1+i\tilde{\eta}_1)\Gamma(1+i\tilde{\eta}_2) \\ &\times \langle\varphi_{12}^-(\mathbf{k}_{12}), \mathbf{K}_{12}\left|\left(V - \frac{\lambda_{12}}{r_{12}}\right)\right|\mathbf{k}_0, \phi_2\rangle\Big], \end{aligned} \tag{1.27}$$

where everything is well defined.

The expression given in (1.27) can now be used to numerically calculate the cross sections. As an example, the results of the cross section calculation based on (1.27) for (e,2e) reactions on a hydrogen atom (solid curve) in comparison with a conventional FBA are presented in Fig. 1. An interesting convergence of theory and experiment is observed in Fig. 2b even in the energy range, where the applicability of the Born approximations is not well justified.

1.4. Concluding Remark to Section 1

In concluding Section 1, which presents material published for the first time in [26], it should be noted that the theory of multiparticle Coulomb scattering enables one to construct a physical ionization amplitude free of extra singularities, as well as to formulate an effective charge method in which those charges are

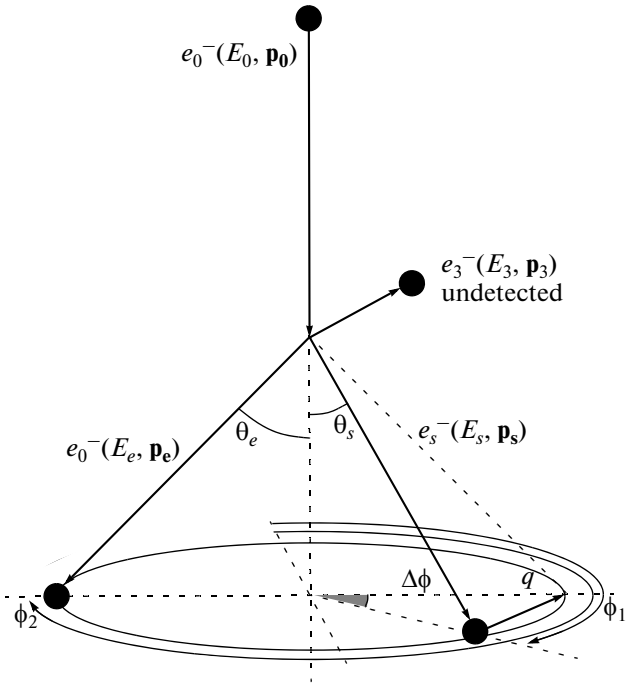

Fig. 2. A diagram of the noncoplanar (e,3e) experiment. The case $\Delta\phi = 0$ corresponds to the plane geometry. The figure is taken from [8].

unambiguously defined, if a Born series is required to be precise up to the second order.

2. TWO FAST PARTICLES IN THE FINAL STATE

2.1. (e,3e) Electron Momentum Spectroscopy

The amplitude matrix elements of multiple ionization of a quantum target by a fast electron, with two fast electrons measured in coincidence in the final state, are the simplest ones from the point of view of a separable representation of the final state function in (I.1). In what follows, we shall consider the helium atom as the simplest two-electron target. In quasi-elastic kinematics the final wave function of a system takes the form of a product of two fast electron plane waves with the momenta $\mathbf{p_s}$, $\mathbf{p_e}$ and the Coulomb wave of a slow electron with the momentum $\mathbf{p_3}$ that describes its free motion in the field of a nucleus with the charge $Z = -2$ [29],

$$|\Psi_f^-(\mathbf{p_s}, \mathbf{p_e}, \mathbf{p_3})\rangle = \frac{1}{\sqrt{2}}[|\mathbf{p_s}, \mathbf{p_e}, \varphi^-(\mathbf{p_3})\rangle + (\mathbf{p_s} \longleftrightarrow \mathbf{p_e})]. \quad (2.1)$$

In its turn the initial wave function is represented as a product of the plane wave of a fast incoming electron and the ground state wave function of a helium atom,

$$|\Psi_i^+(\mathbf{p}_0)\rangle = |\mathbf{p}_0, \Phi_0\rangle. \quad (2.2)$$

In this case the potential of Coulomb interaction between target components and an incoming electron is taken for a perturbative potential,

$$V = v_{01} + v_{02} + v_{0N}. \quad (2.3)$$

Substituting the expressions from (2.1)–(2.3) in (I.1), we obtain

$$T_{fi} = \frac{4\pi}{Q^2}M, \quad M = \int d^3r_1 d^3r_2 \varphi^{-*}(\mathbf{p_3}, \mathbf{r}_2; 2) e^{-i\mathbf{q}\mathbf{r}_1}\Phi_0(\mathbf{r}_1, \mathbf{r}_2), \quad (2.4)$$

where $\mathbf{Q} = \mathbf{p}_0 - \mathbf{p_s}$ and the Coulomb function corresponds to (1.5) with $Z_{eff} = 2$. In the integrand, only the exponentially oscillating term is kept that contains the small momenta $\mathbf{p_3}$ and $_q = \mathbf{p_s} + \mathbf{p_e} - \mathbf{p_0}$. It is the EMS geometry that ensures a small value of the momentum q at large p_0, p_s, and p_e: the plane angles θ_s and θ_e of the momenta $\mathbf{p_s}$ and $\mathbf{p_e}$ with respect to $\mathbf{p}_0$ are approximately equal to $\mp 45°$, and $E_s \sim E_e \sim E_0/2$ (for more detail, see [7]).

The fivefold differential cross section upon taking into account various symmetries and exchanges takes the following form:

$$\frac{d^5\sigma}{dE_s dE_3 d\Omega_s d\Omega_e d\Omega_3} = \frac{8p_s p_e p_3}{(2\pi)^6 p_0} C|M|^2, \quad (2.5)$$

where

$$C = \frac{1}{|\mathbf{p_0} - \mathbf{p_s}|^4} + \frac{1}{|\mathbf{p_0} - \mathbf{p_e}|^4} - \frac{1}{|\mathbf{p_0} - \mathbf{p_s}|^2(|\mathbf{p_0} - \mathbf{p_e}|^2)}.$$

Here it is supposed that a slow electron "differs" from electrons s and e, which is completely justified at $E_s \sim E_e \gg E_3$.

From Eq. (2.4) it is seen that such simplifications cause the integral M to look like a double Fourier transform of the helium atom wave function. By varying the momenta $\mathbf{p}_3$ and $\mathbf{q}$ within reasonable limits, it is possible to obtain valuable information about electronic correlations in the target studying the differential cross section given in (2.5). As follows from the results of [29], this property remains intact even if a slow electron is not measured in coincidence, that is, the expression in (2.5) is integrated over spherical angle Ω_3. The energy of that slow electron is fixed by the conservation law $E_0 + E^{\mathrm{He}} = E_s + E_e + E_3$ ($E^{\mathrm{He}} \approx -2.9037$ is the binding energy of helium atom). Such a process is denoted by (e,3 – 1e).

A diagram of the (e,3 – 1e) experiment with a helium atom target in quasi-elastic kinematics is shown in Fig. 2 [8]. The geometry is noncoplanar, with the plane angles θ_s and θ_e being $\mp 45°$ and the initial energy $E_0 = 2\,080$ eV and $E_s = E_e$. The calculation results for the triple differential cross sections (TDCSs) corresponding to a single ionization that leaves an ion He^+ in the ground state are presented in

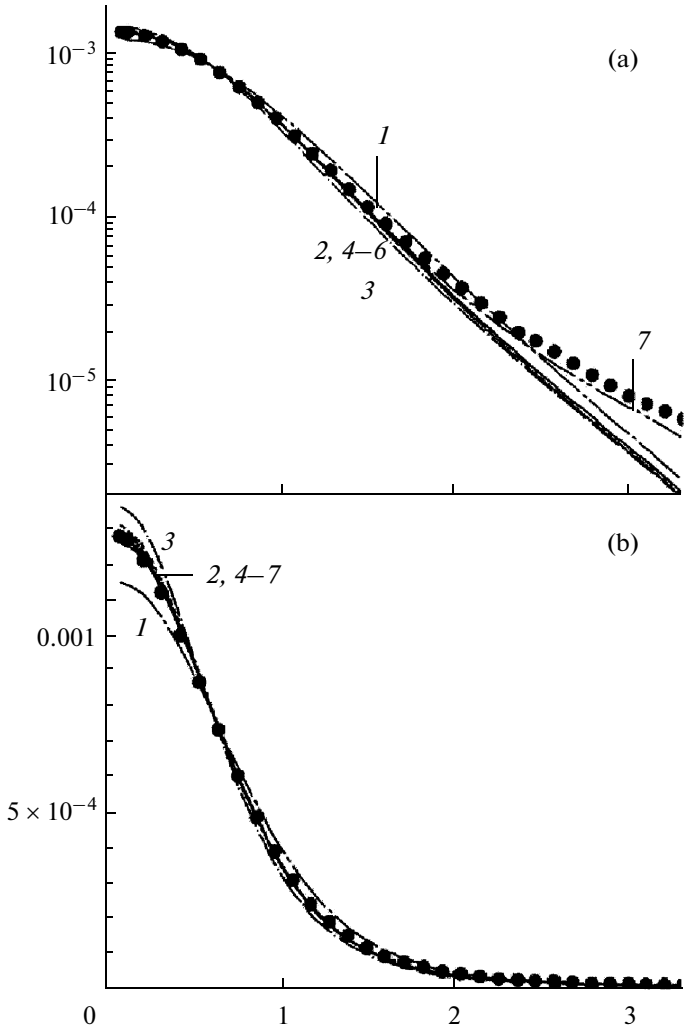

Fig. 3. TDCS of the reaction He + e ⟶ He^+ + 2e in the quasi-elastic kinematics as a function of momentum q. The upper panel (a) is shown in a logarithmic scale, and the lower one (b)—in a linear scale. Curve *1*—Hy × 1.17, *2*—RHF × 1.02, *3*—HEC × 0.94, *4*—CPV × 1.01, *5*—CI × 1.00, *6*—BK × 1.00, *7*—DWBA/CI × 0.79. All theoretical cross sections virtually coincide with each other and the experiment within the limits $q \le 2$ when scaled with the corresponding factors (for details see the text). The figure is borrowed from [8].

Fig. 3 for six trial wave functions of a helium atom. These are the $1s^2$ Hylleraas (Hy) functions [30] ($E^{He}_{Hy} = -2.8477$); Roothaan–Hartree–Fock (RHF) functions [31] ($E^{He}_{RHF} = -2.8617$); Hylleraas–Eckart–Chandrasekhar (HEC) functions with radial correlations [30, 32, 33] ($E^{He}_{HEC} = -2.8757$); 12-component variational Chuluunbaatar–Puzynin–Vinitsky (CPV) functions [34] ($E^{He}_{CPV} = -2.9030$); Mitroy et al. functions in the configuration interaction representation (CI) [35] ($E^{He}_{CI} = -2.9031$); and one of the Bohnam and Kohl (BK) functions [36] ($E^{He}_{BK} = -2.9035$). The explicit expressions for all these functions are gathered in [8]. Furthermore, calculations in the distorted wave approximation (DWBA) were carried out by using both the CI function and the code presented in works by Weigold and McCarthy [37] (see also review [14] and references therein).

The experiments performed by the Japan group [8] do not allow measurements of the cross section absolute values for the processes considered. However, analogous experimental conditions with different states of a final ion lend some credibility to a quasi-absolute scale argument. The idea of quasi-normalization rests on a virtually identical FBA calculation for various trial helium functions in both the form and the absolute magnitude up to $q \sim 2$ [7, 14, 15, 39]. Therefore, the experimental cross section was normalized to the FBA calculations with the use of CI wave function; namely, the area under this theoretical curve was computed up to $q = 1.7$, and the ratio of similar areas for other trial

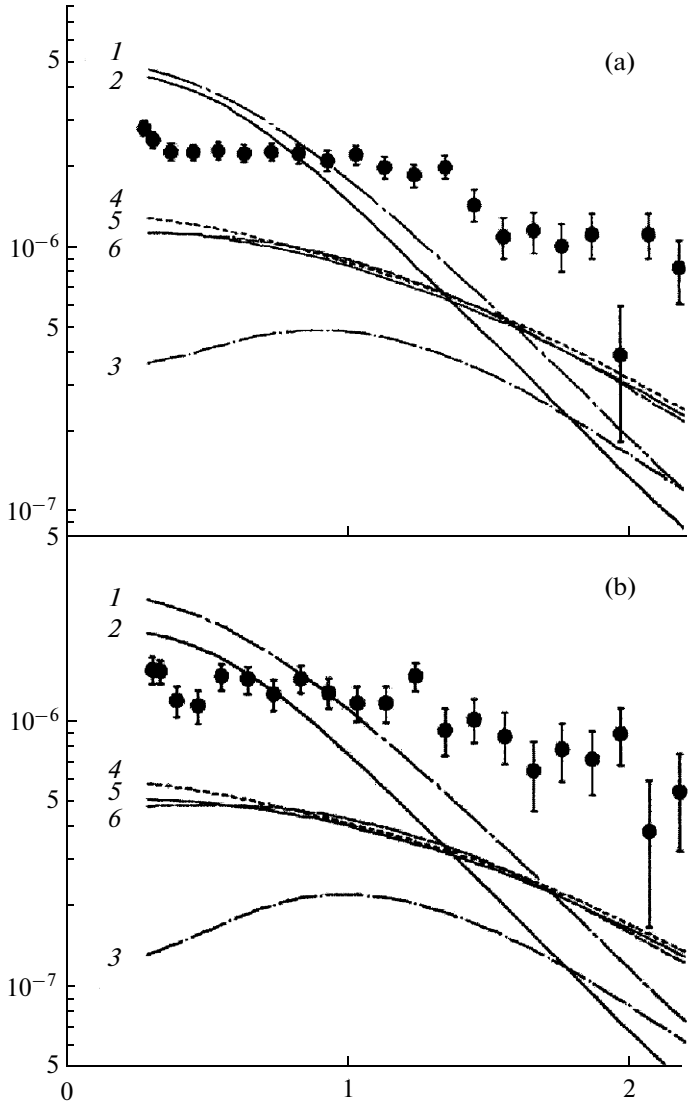

Fig. 4. 4DCS of the reaction He + e ⟶ He^{++} + 3e in the quasi-elastic kinematics as a function of momentum q: $E_3 = 10$ eV (a), $E_3 = 20$ eV (b). An electron e_3 is not detected. Labels are the same as in Fig. 2. The figure is taken from [8].

functions to a given "standard" one determined the individual coefficient for each trial function. The curves of (e,2e) reaction cross sections versus momentum q are presented in the upper panel of Fig. 3 in the logarithmic scale, while in the lower panel they are shown in the linear scale. The computed normalization factor was then used for (e,3 – 1e) processes. In addition to the calculations with the CI function, the cross section calculations with the use of the wave functions Hy, RHF, HEC, CPV, and BK, as well as DWBA calculations, are presented in Fig. 4 scaled by a factor of 1.17, 1.02, 0.94, 1.01, 1.00, and 0.79, respectively. The energy of a slow electron in the upper panel $E_3 = 10$ eV, while in the lower one it is 20 eV.

Unlike Fig. 3, a fairly diverse picture of momentum distributions of (e,3 – 1e) reactions is observed in Fig. 4. Curves obtained by using uncorrelated Hy and RHF $1s^2$ functions give results similar to each other, which strongly differ from the experimental shapes at both energies $E_3 = 10$ and 20 eV. The shape of a simple radially correlated HEC function also fails to match in both the form and quasi-absolute value with the shapes of more advanced trial functions. In turn, the "good" trial functions, with energies close to E^{He}, exhibit (after being multiplied by the corresponding coefficients) shapes that coincide with each other and the experimental shape in form, but differ from the experimental one in the quasi-absolute value by almost a factor of 2. This discrepancy was removed by employing calculations in the second Born approximation (SBA) [40]. Here we will not consider the SBA in detail and would only like to note that the leading contributions come from the excitations of intermediate ion He^+. At this point, it is important to realize that

(e,3 – 1e) quasi-elastic processes not only let the trial wave functions be selected by their binding energies, but also identify a group of seemingly different functions with binding energies close to the experimental ones that produce momentum distributions coinciding with each other.

2.2. Transfer Ionization

Transfer ionization (TI) means an electron capture from the target with simultaneous ionization of the latter by a fast proton (with an energy of a few MeV). It belongs to rearrangement processes (I.2) and can also be related to reactions with two fast particles in the final state (a fast proton and a captured electron). Once again, we take a helium target and consider very small scattering angles of hydrogen produced (parts of mrad) in the reaction $He + p \longrightarrow He^{++} + H + e$. This enables us to assume that the reaction proceeds with relatively small momentum transfer to a helium ion and leaves its nucleus at rest because of a large nucleus mass, i.e., it is possible to take $\mathbf{r}_N \approx 0$ in the laboratory coordinate frame. In this case the final state of a system is approximately written in the form

$$\langle \mathbf{r}_p, \mathbf{r}_1, \mathbf{r}_2 | \Psi_f^-(\mathbf{p}_H, \mathbf{k}) \rangle \approx \frac{1}{\sqrt{2}} [e^{i\mathbf{p}_H\mathbf{r}_p} \phi_H(\mathbf{r}_p - \mathbf{r}_1)\varphi^-(\mathbf{k}, \mathbf{r}_2; 2) + (1 \longleftrightarrow 2)]. \quad (2.6)$$

In this formula $\mathbf{r}_p$, $\mathbf{r}_1$, and $\mathbf{r}_2$ are the radius vectors of a proton and first and second electrons, respectively; $\varphi_H(\mathbf{r})$ is the wave function of a produced hydrogen atom (as a rule, in the ground state); and $\varphi^-(\mathbf{k}, \mathbf{r}_2; 2)$ is the Coulomb wave of a released electron. The initial state of a system is written in a form analogous to (2.2),

$$\langle \mathbf{r}_p, \mathbf{r}_1, \mathbf{r}_2 | \Psi_i^+(\mathbf{p}_p) \rangle = e^{i\mathbf{p}_p\mathbf{r}_p} \Phi_0(\mathbf{r}_1, \mathbf{r}_2). \quad (2.7)$$

Define the momentum transfer $\mathbf{q} = \mathbf{p}_H - \mathbf{p}_p$ and take the potential of Coulomb interaction between the target components and incoming proton to be perturbative,

$$V_i = v_{p1} + v_{p2} + v_{pN}. \quad (2.8)$$

Substituting the expressions given in (2.6)–(2.8) into (I.2), we obtain

$$\mathrm{FBA} = -4\pi\sqrt{2} \int \frac{d\mathbf{x}}{(2\pi)^3} \frac{\tilde{\phi}_H(x)}{|\mathbf{v}_p - \mathbf{q} - \mathbf{x}|^2} \times [F(\mathbf{q}; 0; \mathbf{k}) + F(\mathbf{v}_p - \mathbf{x}; -\mathbf{v}_p + \mathbf{q} + \mathbf{x}; \mathbf{k}) - 2F(\mathbf{v}_p - \mathbf{x}; 0; \mathbf{k})] = \mathrm{A1} + \mathrm{A2} + \mathrm{A3}, \quad (2.9)$$

where for convenience the following notation is introduced:

$$F(\mathbf{y}; \boldsymbol{\eta}; \mathbf{k}) = \int e^{-i\mathbf{y}\mathbf{r}_1 - i\boldsymbol{\eta}\mathbf{r}_2} \varphi^{-*}(\mathbf{k}, \mathbf{r}_2; 2) \times \Phi_0(\mathbf{r}_1, \mathbf{r}_2) d\mathbf{r}_1 d\mathbf{r}_2, \quad (2.10)$$

$\tilde{\phi}_H(x)$ is the hydrogen function in the momentum representation and $\mathbf{v}_p = \mathbf{p}_p/m$ is the proton velocity. The integral A1 is readily calculated analytically,

$$\mathrm{A1} = -\frac{4\sqrt{2\pi}}{1 + (\mathbf{v}_p - \mathbf{q})^2} F(\mathbf{q}; 0; \mathbf{k}), \quad (2.11)$$

while the rest are numerically computed.

The laws of conservation of momentum

$$\mathbf{p}_p = \mathbf{p}_H + \mathbf{k} + \mathbf{K}, \quad (2.12.1)$$

and energy

$$E = \frac{p_p^2}{2m} + E^{He} = \frac{p_H^2}{2(m+1)} + \frac{k^2}{2} + \frac{K^2}{2M} + E^H, \quad (2.12.2)$$

where $\mathbf{K}$ denotes the ion momentum and $M \approx 4m$ is its mass, allow the value of the momentum transfer q to be calculated if the quantity $\mathbf{v}_p$ is taken for the z axis:

$$q_z = \frac{v_p}{2} - \frac{k^2 - 2(E^{He} - E^H)}{2v_p}, \quad q_\perp = m v_p \sin\theta_p \approx m v_p \theta_p. \quad (2.13)$$

From relations (2.12) and (2.13), it is seen that the proton velocity at an energy of several MeV does not exceed 10 atomic units; correspondingly, the value of q_z is of the same order. If the electron energy is taken to be within the limits of even hundreds of keV, then the value of the ion momentum K is also a few atomic units, while the proton mass is $m = 1836.15$. This lets the energy of motion and ion velocity be set precisely equal to zero. As for $q_\perp$, the product $m\theta_p$ does not exceed a unit at scattering angles of up to 0.5 mrad. These considerations specify the characteristic scales of the problem at hand.

Consider now the physical meaning of FBA amplitudes. The amplitude A1 is the so-called plane-wave Oppenheimer–Brinkman–Kramers (OBK) approximation. In the FBA it can be thought of as a proton–electron collision with subsequent capture of the same electron (a fast final electron, although related with a fast incoming particle). A second electron is emitted as a result of instantaneous rearrangement of the potentials in a target atom. This is a typical mechanism of shake off (SO), described, for example, in [41]. Comparison of the expressions presented in (2.11) and (2.4) shows that their integral factors are completely identical, and, seemingly, TI and direct quasi-elastic reactions could successfully complement each other while studying electronic correlations in a target, even more so as the range of q momentum variation in the capture processes is wider. This observation was made in [42]. However, to support this conclusion it is required to estimate the contributions of the A2 and A3 terms.

The amplitude A3 describes tangential (a large impact parameter) collision of heavy particles, followed by electron capture by a proton. In fact, this is

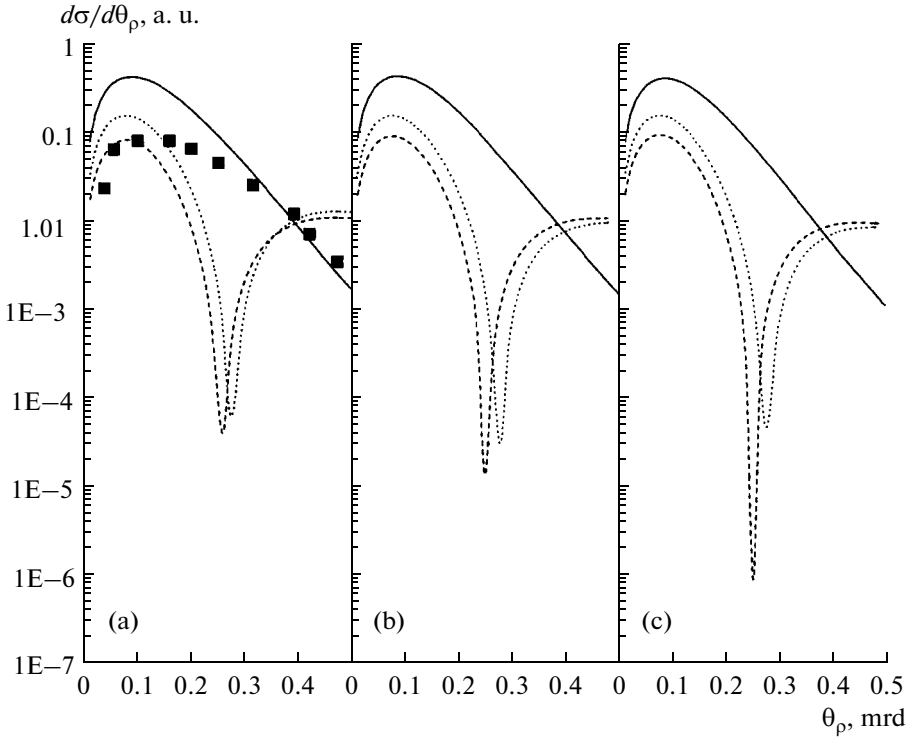

Fig. 5. SDCS of the reaction $He + p \longrightarrow He^+ + H$ as a function of the scattering angle θ_p: Hy (a), RHF (b), CI (c) [35]. Solid curve—A1, dashed curve—A1 + A3, dotted curve—A1 + A2 + A3. The figure is taken from [49].

the SO ionization mechanism as well. The amplitudes A1 and A3 were widely used in earlier calculations of the fast charge exchange processes (CE) (see, e.g., the database compiled in SINP MSU [43]).

Finally, the amplitude A2 describes a process in which a proton collides with some active electron from a target and knocks it out, but captures another active one. In fact, such a scattering process should be attributed to SBA, but here it is part of FBA. The mechanism, when an incoming particle acts in two steps on the system components, is denoted as TS2 and described in [44].

As a rule, in an experiment a single differential cross section (SDCS) is measured in the case of a simple charge exchange (without ionization, with a residual ion He^+ in the ground state),

$$\frac{d\sigma}{d\theta_p} = \frac{m^2\theta_p}{2\pi}|\mathrm{A1} + \mathrm{A2} + \mathrm{A3}|^2, \qquad (2.14)$$

where it is necessary to substitute $\varphi^{-*}(\mathbf{k}, \mathbf{r}_2; 2)$ for $\phi_{He^+}(\mathbf{r}_2)$ in (2.10) and k^2 for $2E^{He^+}$ in (2.13) so as to be able to calculate corresponding amplitudes. Of course, in a real experiment with the possibility of measuring as things as precisely as possible, it is required to take into account excitations of both an ion and a hydrogen, and perform corresponding summations in (2.14) in such a way that this expression is theoretically minimal as compared to the experiment. In addition, the cross section found in (2.14) must be subjected to the so-called convolution operation, since, in a real experiment, the angle is measured on average within some interval, i.e., it is required to average the cross section as well. As a rule, this latter averaging considerably smooths possible spikes in the shape of the cross section. These issues will not be covered in greater detail.

In TI processes it is possible to measure the double differential cross section (DDCS),

$$\frac{d^2\sigma}{d\theta_p d\mathbf{k}} = \frac{m^2\theta_p}{(2\pi)^4}|\mathrm{A1} + \mathrm{A2} + \mathrm{A3}|^2, \qquad (2.15)$$

with the amplitude given in (2.9), as well as various integral variations, e.g., the single differential cross section

$$\frac{d\sigma}{d\theta_p} = \frac{m^2\theta_p}{(2\pi)^4}\int|\mathrm{A1} + \mathrm{A2} + \mathrm{A3}|^2 d\mathbf{k}, \qquad (2.16)$$

when an outgoing electron is not detected. Because of the rapid decrease of the amplitudes with k, increasing the integration in (2.16) is limited by several tens of atomic units. A large amount of experimental data on the capture in coincidence, obtained with a helium target, have been accumulated by Schmidt-Böcking's group [45–48].

SDCS is shown as a function of the scattering angle θ_p in Fig. 5 for three trial helium functions: $1s^2$ func-

tions Hy [30] and RHF [31] and correlated CI function [35]. It is seen that the contributions of the A2 and A3 terms considerably improve matching with the experiment at the angles $\theta_p \le 0.2$ mrad with respect to OBK (A1), with the contribution of the A2 amplitude being relatively small. Calculations are given without a convolution operation being applied, which smooths a dip in the cross section in the vicinity of $\theta_p \sim 0.25$ and provides better agreement between theory and experiment in this region. Moreover, calculations of all three FBA terms are nearly independent of the shape of the helium wave function, as was also observed in the case of (e,2e) EMS experiments (see Fig. 3). Here the leading contribution comes only from the $1s^2$ part of the wave function.

This effect can be explained if one resorts to the coordinate representation of A2 and A3 integrals in the case of simple charge exchange:

$$\mathrm{A3} = 2\sqrt{2}\int d\mathbf{r}_2 \phi_{\mathrm{He}^+}(\mathbf{r}_2) J(\mathbf{r}_2; \mathbf{q}, \mathbf{v_p} - \mathbf{q}), \qquad (2.17)$$

where

$$J(\mathbf{r}_2; \mathbf{q}, \mathbf{v_p} - \mathbf{q}) = \int \frac{d\mathbf{r}_0 d\mathbf{r}_1}{|\mathbf{r}_0 - \mathbf{r}_1|} e^{-i\mathbf{q}\mathbf{r}_1} e^{-i(\mathbf{v_p} - \mathbf{q})\mathbf{r}_0} \times \phi_{\mathrm{H}}(\mathbf{r}_0)\Phi_0(\mathbf{r}_1, \mathbf{r}_2), \qquad (2.18)$$

and

$$\mathrm{A2} = -\sqrt{2}\int \frac{d\mathbf{r}_0 d\mathbf{r}_1 d\mathbf{r}_2}{|\mathbf{r}_0 - \mathbf{r}_1 + \mathbf{r}_2|} e^{-i\mathbf{q}\mathbf{r}_1} e^{-i(\mathbf{v_p} - \mathbf{q})\mathbf{r}_0} \times \phi_{\mathrm{He}^+}(\mathbf{r}_2)\phi_{\mathrm{H}}(\mathbf{r}_0)\Phi_0(\mathbf{r}_1, \mathbf{r}_2). \qquad (2.19)$$

A typical helium CI function (also known as a Slater-type function) has the form

$$\Phi_0(\mathbf{r}_1, \mathbf{r}_2) = \sum_{l=0} \Psi_l(\mathbf{r}_1, \mathbf{r}_2), \qquad (2.20)$$

where

$$\Psi_l(\mathbf{r}_1, \mathbf{r}_2) = 4\pi \sum_{n \ge (l+1)} C_{nl}\psi_{nl}(r_1)\psi_{nl}(r_2) \times \sum_{m=-l}^{l} \langle l, m; l, -m|0, 0\rangle Y_{l,m}(\mathbf{r}_1) Y_{l,-m}(\mathbf{r}_2); \qquad (2.21)$$

$$\psi_{nl}(r) = r^l \sum_i d_i^{ml} \sqrt{\frac{(\varepsilon_i^{nl})^3}{\pi}} e^{-\varepsilon_i^{nl} r}.$$

In particular, the simplest $1s^2$ He wave function is written as follows:

$$\Phi_0(\mathbf{r}_1, \mathbf{r}_2) = \frac{Z^3}{\pi} e^{-Z(r_1 + r_2)}, \quad Z = 27/16 = 1.6875.$$

From general principles of integration of rapidly oscillating functions with some smooth functions and noting that the quantities q, $|\mathbf{v_p} - \mathbf{q}| \gtrsim v_p/2$ in (2.13) and (2.14) are large, it follows that the leading contribution to these integrals comes from the partial terms with $l = 0$ in (2.21). This conclusion is also supported by a numerical integration with only the $1s^2$ term $\Psi_0(\mathbf{r}_1, \mathbf{r}_2)$ in the CI function of Mitroy et al. [35] retained.

The situation dramatically changes if the charge exchange processes with ionization are considered. It turns out that the term A2 in (2.9) makes the leading contribution to the FBA sum regardless of the shape of the trial function. It is interesting to note that, if the electronic correlations are completely "switched off" in the helium wave function, then this is the only term that remains nonzero. The rest will disappear by virtue of the orthogonality of helium ion eigenfunctions that belong to different branches of the spectrum. This is why the $1s^2$ terms in (2.21) here make a rather small contribution to the total FBA amplitude.

SDCS obtained by a numerical integration of the expression given by (2.15) is presented in Fig. 6. Theoretical curves are shown without a convolution operation applied. The curve "tails" at $\theta_p \gtrsim 0.2$ mrad are determined mainly by the A2 amplitude, since the others decrease faster. It is interesting to note that, once again, the cross sections for "good" correlated trial functions coincide, in spite of the dominating reaction mechanism, completely differently from in the case of (e,3e) quasi-elastic reactions, and the integral nature of the cross section given by (2.16). The "bad" Hy function makes an appreciably different contribution.

In Fig. 7 the differential cross section

$$\frac{d^2\sigma}{dE_e d\Omega_e} = \frac{m^2 k}{(2\pi)^5}\int |\mathrm{A1} + \mathrm{A2} + \mathrm{A3}|^2 d\Omega_p, \qquad (2.22)$$

is shown that reflects the distribution of the ionized electron as a function of the emission angle θ_e (see also analogous Fig. 1 in [52]). The calculation is again carried out for the correlated and $1s^2$ trial function. Of course, we fully agree with the discussion of a role played by SBA terms given in the work by Godunov et al. [52] (the region around 100°). However, we would like to draw the reader's attention to the fact that the cross sections calculated with trial wave functions having different levels of electronic correlations can successfully describe different parts of the experimental distribution. This point may give rise to hasty conclusions.

2.3. Discussion of Section 2 Results

Two quite different ionization processes involving a fast incoming particle and a helium atom are considered in Section 2. Strictly speaking, this is a four-body problem. However, the presence of two fast particles in the final state (two electrons in quasi-elastic reactions and a bound (pe)-pair in a capture reaction) makes it possible to substantially simplify the description of the final states of such processes and consider them within an FBA framework. Such reactions are very informa-

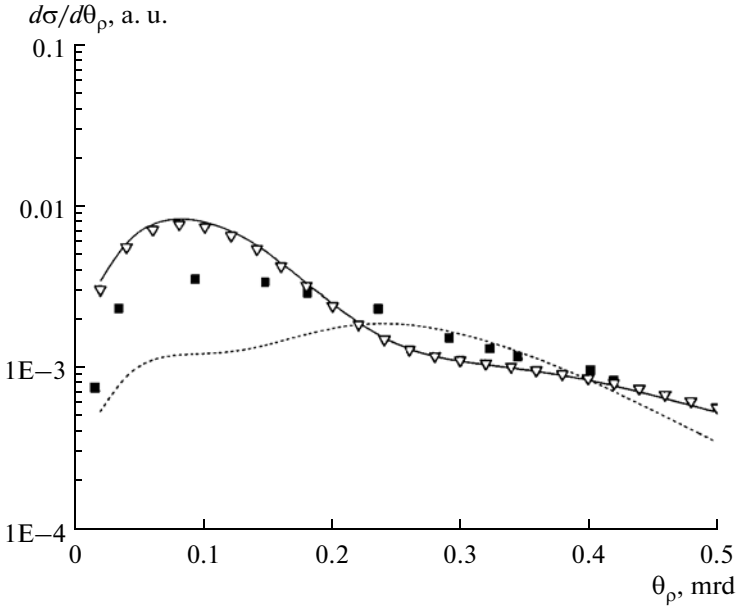

Fig. 6. SDCS of the reaction He + $p \longrightarrow$ He^{++} + H + e as a function of the scattering angle θ_p. Solid curve—CI function by Mitroy et al. [35], triangles—CI function by Nesbet and Watson, dotted curve—Hy function by Hylleraas, black squares—experiment [45]. The figure is borrowed from [51].

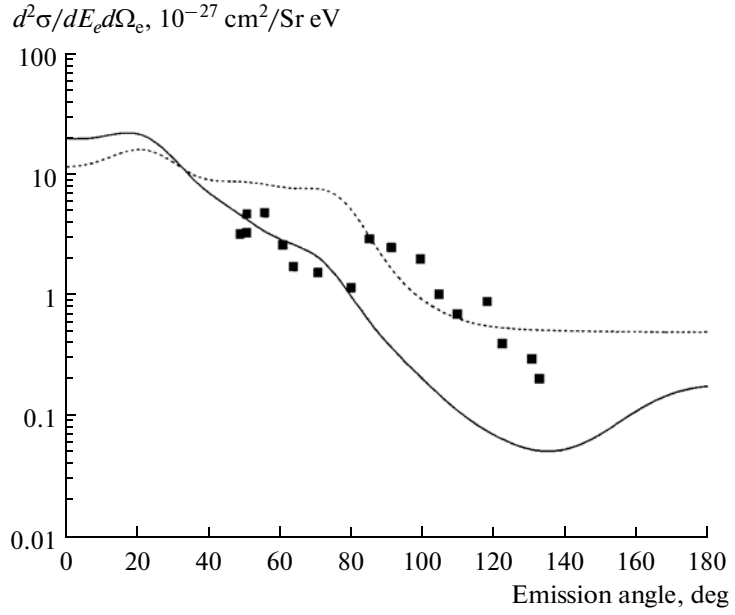

Fig. 7. DDCS of the reaction He + p $\longrightarrow$ He^{++} + H + e as a function of the electron emission angle θ_e: $E_e = 600$ eV, $E_p = 1.0$ MeV. Solid curve—CI function by Mitroy et al. [35], dotted curve—Hy function by Hylleraas, black squares—experiment [53]. The figure is taken from [51].

tive of electronic correlations in a target, even in the case of transfer.

The latter circumstance is quite surprising, since SDCS is a result of multiple integrations of the amplitudes and their sums and, seemingly, information on the fine correlation processes should be leveled. Moreover, here the dominating contribution in FBA amplitude comes from the least "informative" term, A2, which contributes even in the case of entirely missing electronic correlations in a quantum target, rather than from the OBK term, which is completely analogous to the amplitude of (e,3e) quasi-elastic knockout. It should be noted that the fact of rich information content in TI experiments was repeatedly mentioned in the works by the members of Schmidt-Böcking's group [45–48].

In general, we should say that the A2 and A3 amplitudes in both CE and TI reactions admit almost no approximate expressions associated with high velocity of an incoming proton, in addition to those mentioned above. The so-called MPA (the multiple peaking approximation, see, e.g., [54]) does not work already for the angles $\theta_p \gtrsim 1.5$ mrad in the case of CE and completely fails in the case of TI reactions. Some integrals can be analytically evaluated following Lewis [55]. Details can be found in [51]; here we do not intend to further elaborate on this interesting problem.

Unfortunately, the differential cross sections with two fast fragments in the final state are extremely small, on the atomic scale, and decrease rather rapidly with increasing energy of an incident particle. This especially applies to the charge exchange reactions. For this reason, experimenters are not much inclined toward conducting such experiments and, rather, prefer to deal with reactions featuring just one particle in the final state. These latter will be considered in the next section.

3. ONE FAST PARTICLE IN THE FINAL STATE

One particle in the final state is usually a particle, incident on a (neutral) target, that has transferred to it a (small) part of its energy and momentum. Within an FBA framework, factorization of the final function of a system is trivial here: for a sufficiently fast particle, its wave function is in fact the plane wave multiplied by the wave function of the target's final state. Further simplification of this wave function looks problematic, especially at small (near-threshold) energies of emitted electrons, even if there is only one.

A majority of theoretical and experimental works are associated with dipolar reactions on a helium target. In this case, the final wave function describes a three-body continuum of two slow electrons in the field of a nucleus (at rest). As was discussed in the Introduction, even this simple problem does not possess a solution that could be used in numerical calculations. We shall expand on the approaches present here later in this section.

Among the approximations, the so-called 3C-function, which is a product of three functions of the type similar to Eq. (1.5) [56], and several variations thereof ought to be mentioned. Ground-breaking calculations with this function in the case of a helium target were conducted by Dal Capello and Joulakian [57] and showed great sensitivity of the fivefold differential cross section to the correlations among final electrons, while the (e,3e) experiments themselves, in which all three final electrons were measured in coincidence, including the fast one, were carried out by the Lahmam-Bennani group [58]. Moreover, measurements are presented, the authors claim, on an absolute scale, although this statement is still under debate.

Electronic correlations in the final state play an apparently decisive role in dipolar reactions. A striking illustration of this observation that we will consider in the next subsection is the process of multiple ionization of noble gases by a fast electron.

3.1. Multiple Ionization of Noble Gas Atoms by a Fast Electron

The problem of inelastic interaction between the fast charged particle and the atom has a long history and is particularly important for understanding physics of particles and radiations propagating through a medium. The fundamental works in this field were done by Bohr [64] and Bethe [65]. In this subsection we consider n-fold ionization of atom A by the electron impact, with one fast (scattered) and n sufficiently slow (emitted) electrons in the final state. It is natural to represent a final wave function in the following form:

$$|\Psi_f^-(\mathbf{p}_s, \mathbf{k}_1, \mathbf{k}_2, ..., \mathbf{k}_n; A^{n+})\rangle = |\mathbf{p}_s, \Phi_{A^{n+}}^-(\mathbf{k}_1, \mathbf{k}_2, ..., \mathbf{k}_n)\rangle. \quad (3.1)$$

Here $\mathbf{p}_s$ is the momentum of a fast scattered electron, $\Phi_{A^{n+}}^-(\mathbf{k}_1, \mathbf{k}_2, ..., \mathbf{k}_n)$ is the wave function of the target's final state that describes motion of n free slow electrons in the field of A^{n+} ion. In its turn, the initial wave function is represented by a product of the plane wave of a fast incident electron and the wave function of the atom's ground state,

$$|\Psi_i^+(\mathbf{p}_i)\rangle = |\mathbf{p}_i, \Phi_A\rangle. \quad (3.2)$$

In this case the potential of Coulomb interaction of the target components with incoming electron is taken to be the perturbative one,

$$V = \sum_{j=1}^{Z} v_{0j} + v_{0N}, \quad (3.3)$$

where Z denotes the charge of an atom. Substituting expressions (3.2) and (3.3) into (I.1), we obtain

$$T_{fi} = \frac{4\pi}{Q^2} M_n(\mathbf{Q}),$$
$$M_n(\mathbf{Q}) = \langle \Phi_{A^{n+}}^-(\mathbf{k}_1, \mathbf{k}_2, ..., \mathbf{k}_n) \left| \sum_{j=1}^{Z} e^{i\mathbf{Q}\mathbf{r}_j} - Z \right| \Phi_A \rangle, \quad (3.4)$$

where $\mathbf{Q} = \mathbf{p}_i - \mathbf{p}_s$ stands for the momentum transfer to an atom. The differential cross section is written as follows:

$$d\sigma_n = \frac{4p_s}{p_i Q^4} |M_n(\mathbf{Q})|^2 \frac{d\mathbf{k}_1}{(2\pi)^3} \frac{d\mathbf{k}_2}{(2\pi)^3} ... \frac{d\mathbf{k}_n}{(2\pi)^3} d\Omega_s, \quad (3.5)$$

where $p_s = \sqrt{p_i^2 - 2I_n - \sum_{j=1}^{n} k_j^2}$ and I_n is the potential of n-fold atom ionization.In general, the measurement

of the completely differential cross section (3.5) is a very difficult experimental problem. Usually, the total cross section σ_n is measured as a function of the incident electron energy. If an atom is unpolarized, then the cross section $d\sigma_n$ is independent of the azimuthal angle φ_s; hence, $d\Omega_s = 2\pi\sin\theta_s d\theta_s = \pi dQ^2/(p_i p_s)$. Further, averaging over initial atomic states (not considered in what follows) and integrating over the final states of slow electrons yields, for the total cross section,

$$\sigma_n = \frac{8\pi}{p_i^2}\int\limits_{Q_{\min}}^{Q_{\max}} \frac{dQ}{Q^3}\mathcal{M}_n^2(Q), \tag{3.6}$$

where

$$\mathcal{M}_n^2(Q) = \int\frac{d\mathbf{k}_1}{(2\pi)^3}\int\frac{d\mathbf{k}_2}{(2\pi)^3}\ldots\int\frac{d\mathbf{k}_n}{(2\pi)^3}\left|M_n(\mathbf{Q})\right|^2 \tag{3.7}$$

is the generalized oscillator strength for n-fold ionization [22]. The integration limits in (3.6) are approximately taken to be

$$Q_{\min} \simeq \frac{I_n}{p_i}, \quad Q_{\max} \simeq 2p_i - \frac{I_n}{p_i}.$$

In the framework of the Bethe theory, the contribution of only small Q values to the integral in (3.6) is taken into account, while the integral in (3.7) is calculated in the dipole approximation. Omitting details that can be found in [22], we obtain the known asymptotic Bethe formula for the total cross section:

$$\sigma_n = \frac{2\pi}{E_0}\left[\mathcal{M}_n^2\ln\left(\frac{2\tilde{Q}_{\max}^2 E_0}{I_n^2}\right) + \mathbb{O}\left(\frac{1}{E_0}\right)\right], \tag{3.8}$$

where

$$\mathcal{M}_n^2 = \int\frac{d\mathbf{k}_1}{(2\pi)^3}\int\frac{d\mathbf{k}_2}{(2\pi)^3}\ldots\int\frac{d\mathbf{k}_n}{(2\pi)^3} \times\left|\left\langle\Phi^-_{A^{n+}}(\mathbf{k}_1, \mathbf{k}_2, \ldots, \mathbf{k}_n)\middle|\sum_{j=1}^{Z} z_j\middle|\Phi_A\right\rangle\right|^2, \tag{3.9}$$

and $\tilde{Q}_{\max}$ is the momentum parameter in the Bethe theory that limits from above the region of applicability of the dipole approximation. According to Bethe formula (3.8), for reasonably high energy of the incident electron, the quantity $E_0\sigma_n$ should linearly depend on $\ln E_0$ (a so-called Fano plot [66]). The slope of the line calculated is determined by the value of the strength of oscillators (3.9).

The results of measurements for the total cross sections of n-fold ionization of a Ne atom and a Ne^+ ion by electron impact are shown in Figs. 8 and 9, respectively. In general, these are in good agreement with asymptotic Bethe formula (3.8) in the region of sufficiently high energies of an incoming electron. Thus, the Born approximation in the interaction between a fast electron and an atom (or an ion), i.e., single interaction of an electron with a target, turns out to be sufficient even for $n \geq 2$. This is not so obvious considering weak electronic correlations in the example of neon. Indeed, as follows from (3.4), only single ionization is possible in the model of independent electrons.

An alternative to this single ionization mechanism is offered by the successive knockout of electrons from an atom by an incident electron. This mechanism is sketched in Fig. 10. It is clear that, in the case at hand, one refers to the n^{th}-order Born approximation. The corresponding amplitude looks like

$$T_{fi} = \langle\mathbf{p}_s, \Phi^-_{A^{n+}}(\mathbf{k}_1, \mathbf{k}_2, \ldots, \mathbf{k}_n)| \times [VG_0(E)]^{n-1}V|\mathbf{p}_i, \Phi_A\rangle, \tag{3.10}$$

where $G_0(E)$ is the free Green's function, $E = p_i^2/2 = E_A$. If the target electrons are free, then

$$\Phi_A = \frac{1}{\sqrt{Z!}}\hat{A}\prod_{j=1}^{Z}\phi_{i_j}(\xi_j), \tag{3.11.1}$$

$$\Phi^-_{A^{n+}}(\mathbf{k}_1, \mathbf{k}_2, \ldots, \mathbf{k}_n) = \frac{1}{\sqrt{Z}}\hat{A}\left[\prod_{j=1}^{n}\phi(\tilde{k}_j, \xi_j)\right] \times\left[\prod_{j=Z-n+1}^{Z}\phi_{f_j}(\xi_j)\right]. \tag{3.11.2}$$

Here $\hat{A}$ is the antisymmetrization operator; $\tilde{k}_j = (\mathbf{k}_j, \tilde{\mu}_j)$; i_j and f_j denote the sets of single-electron quantum numbers $(nlm\mu)_j$ and $(n'l'm'\mu')_j$ in the initial atomic and final ionic states, respectively; and $\xi_j = (\mathbf{r}_j, \sigma_j)$ is a set of spatial and spin variables for the j^{th} atomic electron. For the energies of atomic and ionic states, we have

$$E_A = \sum_{j=1}^{Z}\varepsilon_{i_j}, \quad E_{A^{n+}} = \sum_{j=Z-n+1}^{Z}\varepsilon_{f_j},$$

where ε_{i_j} and ε_{f_j} are the energies of single-electron states. By substituting (3.11) into (3.10) and using the eikonal approximation [69, 70], we obtain

$$T_{fi} = -ip_i\sum_{\mathcal{P}}(-1)^p\hat{\mathcal{P}}_{i_j}\int d^2b \times\left[\prod_{j=1}^{n}\langle\phi(\tilde{k}_j, \xi_j)\left|\exp[iX(\mathbf{b}; \mathbf{r}_{j,\perp})]\right|\phi_{i_j}(\xi_j)\rangle\right] \times\left[\prod_{j=Z-n+1}^{Z}\langle\phi_{f_j}(\xi_j)\left|\exp[iX(\mathbf{b}; \mathbf{r}_{j,\perp})]\right|\phi_{i_j}(\xi_j)\rangle\right]\exp(i\mathbf{Qb}), \tag{3.12}$$

where $\hat{\mathcal{P}}_{i_j}$ is the operator of all possible permutations of i_j indices, b is the impact parameter, and the eikonal

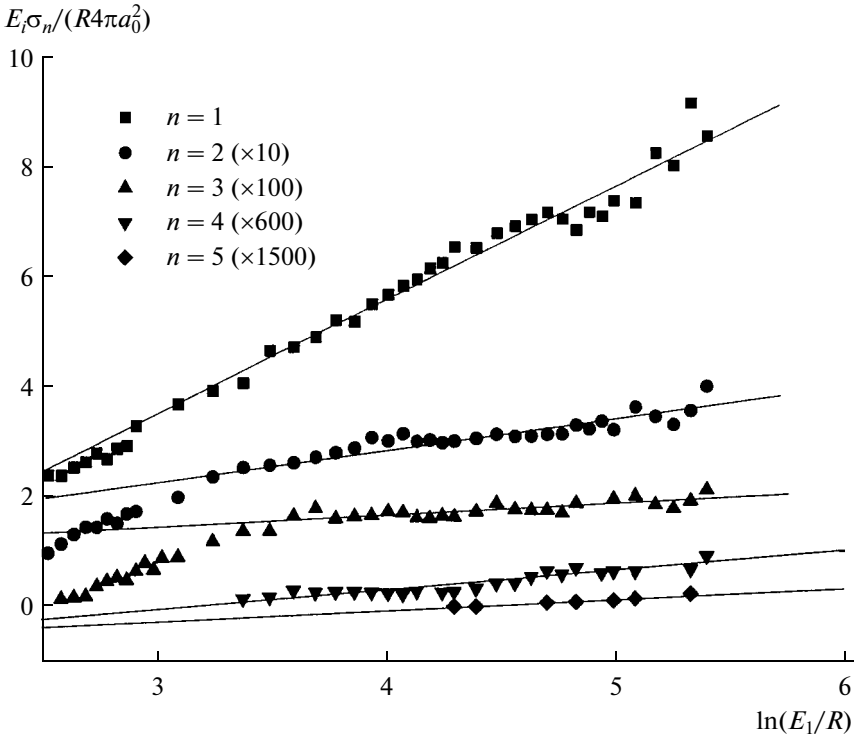

Fig. 8. Fano plot in the case of n-fold ionization of a Ne atom by an electron. The data are taken from [67]. R is the Rydberg constant (27.2 eV), a_0 is the Bohr radius (1 au).

$$X(\mathbf{b};\mathbf{r}_{j,\perp}) = -\frac{1}{p_i}\int_{-\infty}^{\infty} dz_0\left(\frac{1}{|\mathbf{r}_0-\mathbf{r}_j|}-\frac{1}{r_0}\right)$$

$$= -\frac{1}{p_i}\int_{-\infty}^{\infty} dz_0\left(\frac{1}{\sqrt{(\mathbf{b}-\mathbf{r}_{j,\perp})^2+(z_0-z_j)^2}}-\frac{1}{\sqrt{b^2+z_0^2}}\right) \quad (3.13)$$

$$= -\frac{2}{p_i}\ln\frac{b}{|\mathbf{b}-\mathbf{r}_{j,\perp}|}$$

(see, for example, [69]).

Taking into account that $1/p_i \ll 1$, we can write, to a certain approximation,

$$\exp[iX(\mathbf{b};\mathbf{r}_{j,\perp})] \simeq 1 + iX(\mathbf{b};\mathbf{r}_{j,\perp})$$

and keep in (3.12) only nonzero terms of lower order in p_i^{-1}. In this way, we derive

$$T_{fi} = -i^{n+1}p_i\sum_{\mathcal{P}}(-1)^p\hat{\mathcal{P}}_{i_j}\int d^2b$$

$$\times\left[\prod_{j=1}^{n}\langle\phi(\tilde{k}_j,\xi_j)|X(\mathbf{b};\mathbf{r}_{j,\perp})|\phi_{i_j}(\xi_j)\rangle\right] \quad (3.14)$$

$$\times\left[\prod_{j=Z-n+1}^{Z}\delta_{f_j i_j}\right]\exp(i\mathbf{Qb}).$$

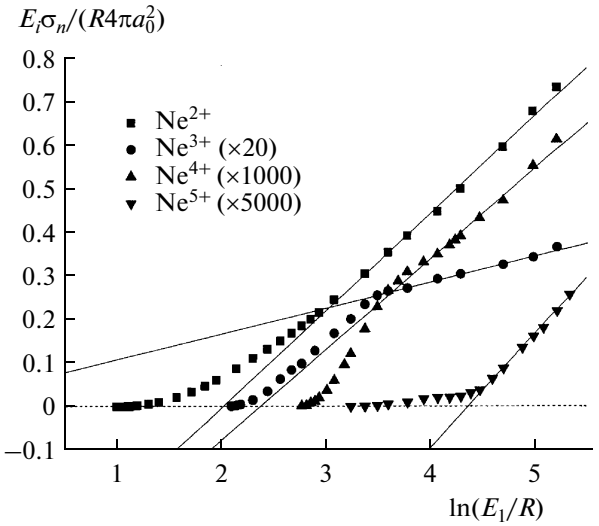

Fig. 9. Fano plot in the case of n-fold ionization of a Ne^+ ion by an electron. The data are taken from [68].

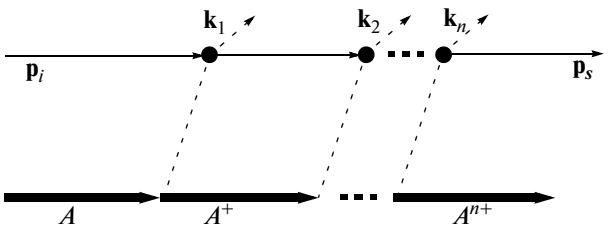

Fig. 10. Ladder diagram corresponding to successive electron stripping from an atom by an incident electron.

Making use of (3.14) in the total cross section calculation yields

$$\sigma_n = \frac{2\pi}{p_i^{2n-1}} \sum_{\tilde{\mu}_1, \tilde{\mu}_2, \ldots, \tilde{\mu}_n} \int \frac{d^3Q}{(2\pi)^3} \int \frac{d^3k_1}{(2\pi)^3} \times \int \frac{d^3k_2}{(2\pi)^3} \ldots \int \frac{d^3k_n}{(2\pi)^3} \int d^2b \int d^2b', \sum_{\mathcal{P}} (-1)^{p+p'} \hat{\mathcal{P}}_{i_j} \hat{\mathcal{P}}_{i'_j} \left[\prod_{j=1}^{n} u_{i_j i'_j}(\tilde{k}_j) \right] \left[\prod_{j=Z-n+1}^{Z} \delta_{i_j i'_j} \right] \times \exp[i\mathbf{Q}(\mathbf{b}-\mathbf{b}')] \delta\left(p_i Q_z + \sum_{j=1}^{n} \varepsilon_{i_j} - \frac{Q^2}{2} - \sum_{j=1}^{n} \frac{k_j^2}{2} \right), \quad (3.15)$$

where

$$u_{i_j i'_j}(\tilde{k}_j) = \delta_{\tilde{\mu}_j \mu'_j} \delta_{\tilde{\mu}_j \mu_j} \left\langle \phi_{(n'l'm'_l)_j} \left| \ln \frac{b'^2}{|\mathbf{b}' - \mathbf{r}'_{j,\perp}|} \right| \phi^-(\mathbf{k}_j) \right\rangle \times \left\langle \phi^-(\mathbf{k}_j) \left| \ln \frac{b^2}{|\mathbf{b} - \mathbf{r}_{j,\perp}|^2} \right| \phi_{(nlm_l)_j} \right\rangle. \quad (3.16)$$

Integration over Q_z in the limit of large p_i followed by that over $\mathbf{Q}_\perp$ and b' leads to the following expression:

$$\sigma_n = \frac{1}{(2E_0)^n} \sum_{\tilde{\mu}_1, \tilde{\mu}_2, \ldots, \tilde{\mu}_n} \int d^2b \times \sum_{\mathcal{P}} \hat{\mathcal{P}}_{i_j} \left[\prod_{j=1}^{n} \delta_{\tilde{\mu}_j \mu_j} w_{(nlm_l)_j} \right], \quad (3.17)$$

where

$$w_{(nlm_l)_j} = \int \frac{d^3k}{(2\pi)^3} \left| \left\langle \phi^-(\mathbf{k}) \left| \ln \frac{b^2}{|\mathbf{b} - \mathbf{r}_\perp|^2} \right| \phi_{(nlm_l)_j} \right\rangle \right|^2.$$

Note that in (3.17) we omitted interference terms, which is equivalent to neglecting the antisymmetrization procedure [71].

As follows from (3.17), the total cross section of n-fold ionization in the framework of the mechanism of successive electron knockout from an atom behaves like $\sim E_0^{-n}$. This result apparently contradicts both the Bethe formula in (3.8) and experimental observations even in the case of such a weakly correlated system as a neon atom. This conclusion forces us to assume that there are strong correlations among slow electrons in the final state of the reaction, which calls for a dedicated examination. An attempt at such a study was made in [72] within the framework of the effective charge method and looks effective, although still complicated if it were to be carried out in actual calculations.

3.2. 3C-function and Associated Calculations

Let us take $n = 2$ in (3.4). The principal part of the matrix element in this case takes the form

$$M_2(\mathbf{Q}) = \langle \Phi^-(\mathbf{k}_1, \mathbf{k}_2) | e^{i\mathbf{Q}\mathbf{r}_1} + e^{i\mathbf{Q}\mathbf{r}_2} - 2 | \Phi_0 \rangle. \quad (3.18)$$

The exact functions of the initial and final states must be orthogonal $\langle \Phi^-(\mathbf{k}_1, \mathbf{k}_2) | \Phi_0 \rangle = 0$ since they belong to different parts of the spectrum of the same Hamiltonian. The approximate functions in FBA can be orthogonalized by the Gram method, leading to the replacement of the factor of 2 in transition operator (3.18) by $2F(Q)$, where $F(Q) = \langle \Phi_0 | e^{i\mathbf{Q}\mathbf{r}} | \Phi_0 \rangle$ is the so-called atomic form factor.

The nonsymmetrized 3C function is written as follows:

$$\Phi_{3C}^{-*}(\mathbf{k}_1, \mathbf{k}_2; \mathbf{r}_1, \mathbf{r}_2) = e^{i\mathbf{k}_{12}\mathbf{r}_{12}} \varphi^{-*}(\mathbf{k}_1, \mathbf{r}_1; 2) \times \varphi^{-*}(\mathbf{k}_2, \mathbf{r}_2; 2) \varphi_{12}^{-*}(\mathbf{k}_{12}, \mathbf{r}_{12}; -1/2), \quad (3.19)$$

with the Coulomb wave functions defined in (1.5). This function enables us to reduce considerably a number of integrations in 6D matrix element (3.18) for two cases of trial helium atom functions: the Slater-type function and that with correlations explicitly defined by means of the combination r_{12}. Let us take a closer look at this latter case.

Let us define the trial wave function of a helium atom in the following manner:

$$\Phi_{\text{corr}}(\mathbf{r}_1, \mathbf{r}_2) = \sum_j D_j [\exp(-\alpha_j r_1 - \beta_j r_2) + \exp(-\alpha_j r_2 - \beta_j r_1)] \exp(-\gamma_j r_{12}). \quad (3.20)$$

A mechanism for calculating the integral given in (3.18) with the BK function [36] is presented in [59], while the details of the evaluation of such a function, which yields the binding energy $E_{\text{corr}}^{\text{He}} = -2.90372$ and, additionally, satisfies the Kato conditions [60] in a variational form, can be found in [61]. We now introduce an auxiliary function,

$$g_j^*(\mathbf{k}_{12}, \mathbf{k}) = \int d^2 r_{12} e^{i(\mathbf{k}+\mathbf{k}_{12})\mathbf{r}_{12}} e^{-\gamma_j r_{12}} \times \varphi^{-*}(\mathbf{k}_{12}, \mathbf{r}_{12}; -1/2) \quad (3.21)$$

and write

$$M_2(\mathbf{Q}) = \sum_j D_j \int \frac{d^3k}{(2\pi)^3} g_j^*(\mathbf{k}_{12}, \mathbf{k}) \times \int d^3r_1 d^3r_2 e^{-i\mathbf{k}\mathbf{r}_1} e^{i\mathbf{k}\mathbf{r}_2} \varphi^{-*}(\mathbf{k}_1, \mathbf{r}_1; 2) \varphi^{-*}(\mathbf{k}_2, \mathbf{r}_2; 2) (e^{i\mathbf{Q}\mathbf{r}_1} + e^{i\mathbf{Q}\mathbf{r}_2} - 2) \times (e^{-a_j r_1 - b_j r_2} + e^{-a_j r_2 - b_j r_1}). \quad (3.22)$$

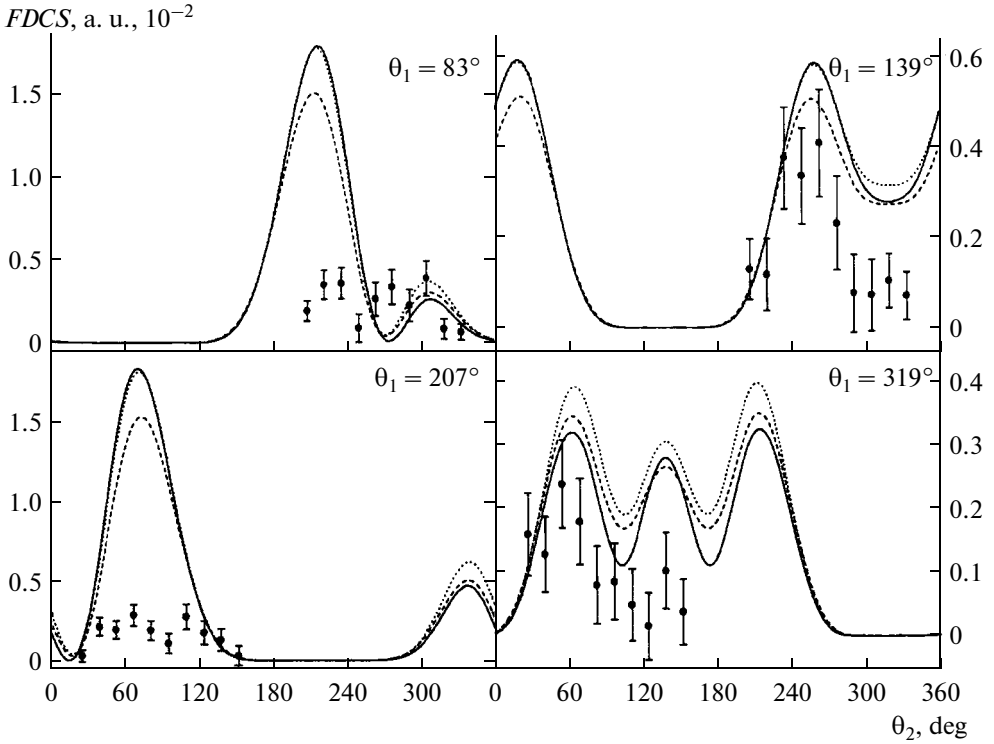

Fig. 11. FDCS dependence on the electron emission angle θ_2 at fixed θ_1 angles. Electron energies are $E_1 = E_2 = 10$ eV, $E_s = 5500$ eV. Solid curve shows results of calculations according to function (3.20), dashed curve—with BK function [63], and dotted curve—with Le Sech function [62]. Experimental points are taken from [58]. The figure is taken from [61].

This allows obtainment of the following expression for the matrix elements, this time in the form of a 3D integral:

$$M_2(\mathbf{Q}) = -\sum_j D_j \frac{\partial^3}{\partial\alpha_j\partial\beta_j\partial\gamma_j}\int\frac{d^3k}{(2\pi)^3} I_{12}(\gamma_j;\, \mathbf{k}_{12}, \mathbf{k}+\mathbf{k}_{12}) \times [I_1(\alpha_j;\mathbf{k}_1, \mathbf{Q}-\mathbf{k}) I_2(\beta_j;\mathbf{k}_2, \mathbf{k}) + I_1(\alpha_j;\mathbf{k}_1, -\mathbf{k}) I_2(\beta_j;\mathbf{k}_2, \mathbf{Q}+\mathbf{k}) - 2I_1(\alpha_j;\mathbf{k}_1, -\mathbf{k}) I_2(\beta_j;\mathbf{k}_2, \mathbf{k}) + (a_j \longleftrightarrow b_j)], \quad (3.23)$$

where

$$I_\tau(\lambda;\mathbf{k}_\tau, \mathbf{k}) = \int\frac{d^3r}{r}\varphi^{-*}(\mathbf{k}_\tau, \mathbf{r};\tau)e^{-\lambda r + i\mathbf{kr}} = 4\pi R(\xi_\tau)\frac{[(\lambda - ik_\tau)^2 + k^2]^{i\xi_\tau}}{[(\mathbf{k}-\mathbf{k}_\tau)^2 + \lambda^2]^{1+i\xi_\tau}}. \quad (3.24)$$

In (3.24) $\tau = 1, 2, (12)$; $\xi_1 = -2/k_1$; $\xi_2 = -2/k_2$; and $\xi_{12} = 1/2k_{12}$ are the Coulomb numbers and $R(\xi) = e^{-\pi\xi/2}\Gamma(1 + i\xi)$.

The fivefold differential cross section (FDCS, 5DCS) with functions (3.19) and (3.20) is written in FBA as follows:

$$\frac{d^5\sigma}{dE_a dE_b d\Omega_a d\Omega_b d\Omega_s} = \frac{8p_s k_1 k_2}{(2\pi)^6 p_i Q^4}|M_2|^2, \quad (3.25)$$

with associated calculations presented in Fig. 11 and compared to the experimental data [58]. Let us recollect that the experimental geometry is plane; the initial electron energy is $E_0 = 5599$ eV; and the energy and angle of a scattered electron are $E_s = 5500$ eV and $\theta_s = -0.45°$, respectively, while the energies of the emitted electrons are $E_1 = E_2 = 10$ eV. As is seen from the figure, the results for all three trial (relatively "good") functions are close to each other regardless of whether the Kato conditions are satisfied exactly [62], integrally [61], or just approximately [36]. There also are sizable discrepancies between all the calculations and the experiment for the angles $\theta_1 = 83°$ and 207°, which can be understood as deriving from the poor quality of the final state function.

So far, we have proceeded from the approximation for the finite wave function quoted in (3.1), that is, described a scattered electron using the plane wave within a finite four-body state. A nonperturbative approach to the final state description can be realized in the 6C model represented as a product of six Coulomb functions in the following way (cf. (3.19)):

$$\Phi_{6C}^{-*}(\mathbf{p}_s, \mathbf{k}_1, \mathbf{k}_2;\, \mathbf{r}_0, \mathbf{r}_1, \mathbf{r}_2) = e^{i\mathbf{k}_{12}\mathbf{r}_{12}} e^{i\mathbf{k}_{1s}\mathbf{r}_{10}} e^{i\mathbf{k}_{2s}\mathbf{r}_{20}} \times \varphi^{-*}(\mathbf{p}_s, \mathbf{r}_0;\, 2)\varphi^{-*}(\mathbf{k}_1, \mathbf{r}_1;\, 2)\varphi^{-*}(\mathbf{k}_2, \mathbf{r}_2;\, 2) \times \varphi_{12}^{-*}(\mathbf{k}_{12}, \mathbf{r}_{12};\, -1/2)\varphi_{1s}^{-*}(\mathbf{k}_{1s}, \mathbf{r}_{10};\, -1/2) \times \varphi_{2s}^{-*}(\mathbf{k}_{2s}, \mathbf{r}_{20};\, -1/2). \quad (3.26)$$

The numerical calculations with this function are extremely complicated and, therefore, seldom carried out in practice (see, e.g., [73]). The effective charge method taken along with the concept of dynamic screening [74] provides a way to get around these computational difficulties. The total interaction potential is represented in the form ($Z_T = 2$):

$$-\frac{Z_T}{r_0}-\frac{Z_T}{r_1}-\frac{Z_T}{r_2}+\frac{1}{r_{10}}+\frac{1}{r_{20}}+\frac{1}{r_{12}} = -\frac{Z_1}{r_1}-\frac{Z_2}{r_2}+\frac{Z_{12}}{r_{12}}, \quad (3.27)$$

where Z_1, Z_2, and Z_{12} are the effective charges to be defined. The procedure of finding these effective charges is given in [74]; here, we only cite the final result:

$$Z_{1,2} = Z_T + \frac{Z_T k_{1,2}}{2 p_s} - \frac{k_{1,2}}{|\mathbf{k}_{1,2}-\mathbf{p}_s|}, \quad Z_{12} = 1. \quad (3.28)$$

Thus, 6C function (3.26) reduces to the 3C one with charges (3.28). (By the way, it is this scheme that was applied in the theoretical analysis of experiments conducted by the Lahmam-Bennani group [58] mentioned earlier.)

3.3. Discussion of Section 3 Results

In the case of just one fast particle in the final state, even if we approximate its wave function by the plane wave, there still remain considerable difficulties in approximating the finite function of a target with a few slow electrons. The effective charge method, as was found in Section 1, allows for removal of a scattering amplitude singularity in the momentum representation obtained from the solution to the Lippmann–Schwinger equation in the plane wave basis, but, in the coordinate representation, the asymptote of the wave function of three-body dissociation, which can be written in the following way:

$$\Psi^{(\pm)}(\mathbf{k}_1, \mathbf{k}_2; \mathbf{r}_1, \mathbf{r}_2)\big|_{r_1, r_2, r_{12}\to\infty} \sim e^{i(\mathbf{r}_1\mathbf{k}_1 + \mathbf{r}_2\mathbf{k}_2 + W^{\pm})} \quad (3.29)$$

with the phase

$$W^{\pm} = \mp\frac{Z}{k_1}\ln(k_1 r_1 \mp \mathbf{k}_1\mathbf{r}_1) \mp \frac{Z}{k_2}\ln(k_2 r_2 \mp \mathbf{k}_2\mathbf{r}_2) \pm \frac{1}{2k_{12}}\ln(k_{12} r_{12} \mp \mathbf{k}_{12}\mathbf{r}_{12}), \quad (3.30)$$

does not formally correspond to the coordinate asymptote of a product of Coulomb functions (1.4) conditioned by (1.3), which is easily verified. At the same time, it is often convenient and customary to start with the coordinate representation, especially in the numerical evaluations.

The 3C function has asymptotic form (3.29) that distinguishes it from the effective charge method, but this function is strictly asymptotic and cannot be a free term for an equation with a local short-range potential for the wave function $|\Psi^{(\pm)}(\mathbf{k}_1, \mathbf{k}_2)\rangle$ (see, for example, [75]). However, recently a series of works have appeared that indicate the route to follow in solving this problem [76, 77].

At the same time, in the course of multiple ionization with $n > 2$, an amazing effect, from our point of view, is observed, when such a number of electrons originating from the ionization process itself appear in FBA. As a matter of fact, FBA is a sum of matrix elements, with each of the latter describing a single interaction of a fast particle with target components. It turns out that one slow emitted electron "pulls out" the remaining ones by virtue of internal correlations only. These, in general, are Coulomb correlations in the final state. This effect needs to be further studied with great attention.

4. MOLECULE IONIZATION BY ELECTRON IMPACT: APPROXIMATIONS

During the last 30–40 years, molecular physics was constantly gaining its realm in quantum scattering theory. The theory of singly ionized molecules effected by a fast particle is extremely complicated; even in the simplest case of a hydrogen molecule, we have to deal with a quantum system of five bodies (with the exception of photoionization). It is nearly impossible to cope with the problem without having it approximated in any reasonable way, even in the numerical evaluations within FBA.

In the case of ionization of a hydrogen molecule with simultaneous dissociation, the registration of both scattered and emitted electrons, as well as one of the protons, can give exclusive information on the target electronic structure and mechanisms of ionization and dissociation. Such a type of detection "in coincidence" is discussed in, e.g., [78–80], devoted to studying the collisions of hydrogen molecules and charged ions (see also references therein). Here as well appears an opportunity to investigate the dependence of the angular differential cross section on the molecule orientation [81].

One of the main difficulties of mathematical simulation of such experiments is in the correct description of continuous spectrum states of emitted electrons moving in the Coulomb field of two nuclei (for instance, two protons—the nuclei of hydrogen molecules). Over the past few years, a number of models were proposed for describing the dynamics of one slow emitted electron in the dipole (e,2e) experiment. For example, in [82] the approximate single-parametric wave function represented as a product of two Coulomb functions in the field of a fixed (as compared to the effective reaction time) center H_2^{++} (the so-called 2C approximation) is used for the reaction $H_2^+ + e \longrightarrow H^+ + H^+ + e + e$. In other theoret-

ical works purely numerical results were obtained by using the method of wave packet evolution in spherical [83] and prolate spheroid coordinates [84, 85]. These methods yield differential cross sections close to each other and quite different from those calculated by the 2C method. However, the use of spheroid functions to expand a plane wave for a given direction of scattered electron momentum requires summation of a large number of partial solutions in the calculations of ionization cross sections, which leads to the cumbersome and slowly converging calculations, thus posing a problem of finding more effective approximation to the reaction's final state function. Let us consider this topic at greater length (based mainly on doctoral dissertation [90]).

4.1. General Formulas

The processes of single and double ionizations of two-atomic molecule with two active electrons by incident fast electron satisfy the laws of conservation of momentum and energy:

$$\mathbf{K} = \mathbf{p}_i - \mathbf{p}_s - \mathbf{k}_1, \quad E_i = E_s + E_1 + I_1, \qquad (4.1.1)$$

$$\mathbf{K} = \mathbf{p}_i - \mathbf{p}_s - \mathbf{k}_1 - \mathbf{k}_2, \quad E_i = E_s + E_1 + E_2 + I_2. \qquad (4.2.2)$$

Here $(E_i, \mathbf{p}_i)$, $(E_s, \mathbf{p}_s)$, $(E_1, \mathbf{k}_1)$, and $(E_2, \mathbf{k}_2)$ are the energies and momenta of incoming, scattered, and emitted electrons, respectively; $\mathbf{Q}$ is the ion recoil momentum; and I_1 and I_2 denote the potentials of single and double ionization of a molecule.

The diagrams of the electron velocity and molecule orientation vectors are shown in Fig. 12. Here $\mathbf{R}$ is the radius vector of a fast scattered electron; $\mathbf{r}_1$ and $\mathbf{r}_2$ are the radius vectors of emitted electrons; $\boldsymbol{\rho}$ stands for the radius vector that connects nuclei a and b of two-atomic molecule and fixes orientation of the axis which a molecule rotates around; $\mathbf{R}_a$, $\mathbf{R}_b$ and $\mathbf{r}_{ja}$, $\mathbf{r}_{jb}$ are the radius vectors of incident and j^{th} emitted electrons relative to nuclei a and b, respectively; $\mathbf{r}_{jp}$ is the radius vector of incident electron relative to the j^{th} emitted one; and $\mathbf{Q} = \mathbf{p}_i - \mathbf{p}_s$ is the momentum transfer. From Fig. 12 it is seen that

$$\begin{aligned} \mathbf{R}_a &= \mathbf{R} + \boldsymbol{\rho}/2, \quad \mathbf{r}_{1p} = \mathbf{R} - \mathbf{r}_1, \\ \mathbf{r}_{1a} &= \mathbf{r}_1 + \boldsymbol{\rho}/2, \quad \mathbf{r}_{2a} = \mathbf{r}_2 + \boldsymbol{\rho}/2, \end{aligned} \qquad (4.2.1)$$

$$\begin{aligned} \mathbf{R}_b &= \mathbf{R} + \boldsymbol{\rho}/2, \quad \mathbf{r}_{2p} = \mathbf{R} - \mathbf{r}_2, \\ \mathbf{r}_{1b} &= \mathbf{r}_1 + \boldsymbol{\rho}/2, \quad \mathbf{r}_{2b} = \mathbf{r}_2 + \boldsymbol{\rho}/2. \end{aligned} \qquad (4.2.2)$$

Triple and fivefold differential cross sections (TDCS and 5DCS) of (e,2e) and (e,3e) reactions with one fast (initial) electron for a fixed molecule orientation within an FBA framework are given by the following expressions:

$$\sigma^{(3)}(\boldsymbol{\rho}) = \frac{d^3\sigma}{d\Omega_s d\Omega_1 dE_1} = \frac{p_s k_1}{(2\pi)^5 p_i}\left|T_{fi}\right|^2, \qquad (4.3.1)$$

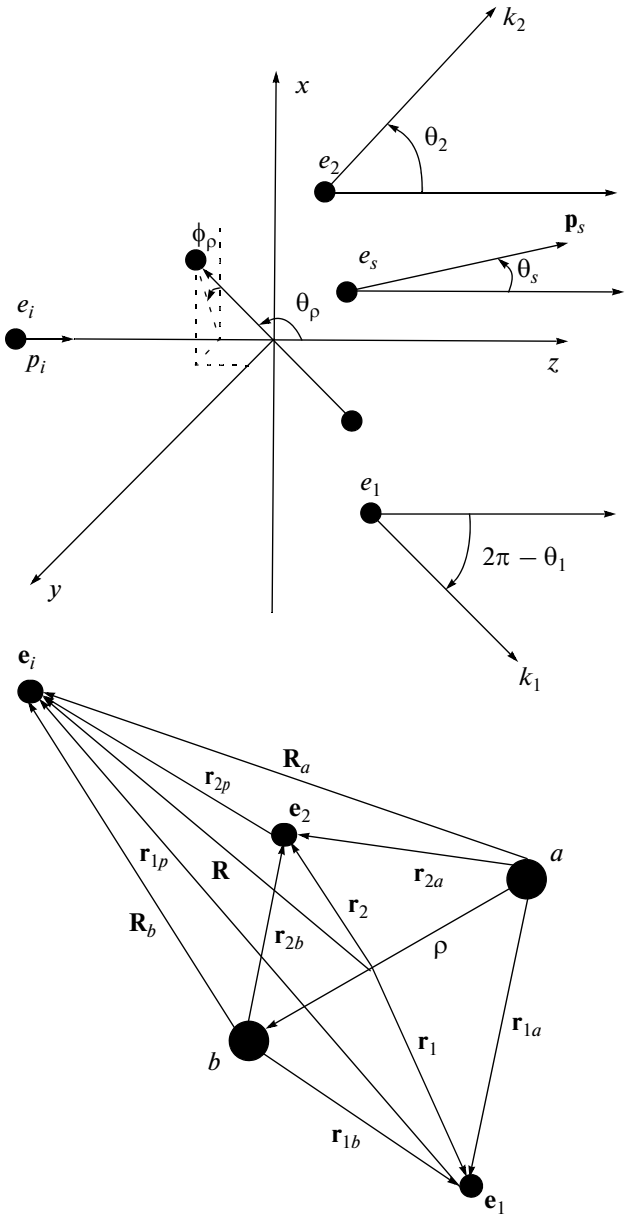

Fig. 12. Diagrams of the velocity vectors (in the laboratory coordinate system) and electron coordinates (in the molecular reference frame).

$$\sigma^{(5)}(\boldsymbol{\rho}) = \frac{d^5\sigma}{d\Omega_s d\Omega_1 d\Omega_2 dE_1 dE_2} = \frac{p_s k_1 k_2}{(2\pi)^8 p_i}\left|T_{fi}\right|^2. \qquad (4.3.2)$$

As usual, in the case of one fast particle, we neglect exchange between incident and emitted electrons and assume that the probability of fast particle capture by a target, followed by the emission of two active electrons, is extremely small. Integrating over all possible

directions of the molecule's axis we obtain the averaged triple and fivefold differential cross sections:

$$\bar{\sigma}^{(3)} = \frac{1}{4\pi}\int d\Omega_\rho \sigma^{(3)}(\boldsymbol{\rho}), \quad (4.4.1)$$

$$\bar{\sigma}^{(5)} = \frac{1}{4\pi}\int d\Omega_\rho \sigma^{(5)}(\boldsymbol{\rho}). \quad (4.4.2)$$

4.2. Target with One Active Electron

Let us consider the Schrödinger equation for the j^{th} emitted electron moving in the field of two nuclei at rest with charges Z_a and Z_b:

$$\left(H - \frac{k^2}{2}\right)\Psi(\mathbf{k}, \mathbf{r}) = 0,$$
$$H = -\frac{1}{2}\Delta_{\mathbf{r}} - \frac{Z_a}{r_a} - \frac{Z_b}{r_b}, \quad (4.5)$$

where $\mathbf{k} \equiv \mathbf{k}_j$, $\mathbf{r} \equiv \mathbf{r}_j$, and $\mathbf{r}_l \equiv \mathbf{r}_{jl}$, $l = a, b$. Its solution will be sought in the form of a product of two functions:

$$\Psi(\mathbf{k}, \mathbf{r}) = \Psi_a(\mathbf{k}, \mathbf{r}_a)\Psi_b(\mathbf{k}, \mathbf{r}_b),$$
$$\Psi_l(\mathbf{k}, \mathbf{r}_l) = \exp\left(\frac{i\mathbf{k}\mathbf{r}_l}{2}\right)\psi(\mathbf{k}, \mathbf{r}_l), \quad (4.6)$$

which was inspired by ideas from the effective charge method. Substituting the function given in (4.6) into Eq. (4.5), we obtain the following equation:

$$\left[\frac{1}{2}\Delta_{\mathbf{r}_a}\psi(\mathbf{k}, \mathbf{r}_a) + \left(i\mathbf{k} + \beta_a\frac{\nabla_{\mathbf{r}_b}\psi(\mathbf{k}, \mathbf{r}_b)}{2\psi(\mathbf{k}, \mathbf{r}_b)}\right)\right.$$
$$\left.\times\nabla_{\mathbf{r}_a}\psi(\mathbf{k}, \mathbf{r}_a) + \frac{Z_a}{r_a}\psi(\mathbf{k}, \mathbf{r}_a)\right]\psi(\mathbf{k}, \mathbf{r}_b)$$
$$+\left[\frac{1}{2}\Delta_{\mathbf{r}_b}\psi(\mathbf{k}, \mathbf{r}_b) + \left(i\mathbf{k} + \beta_b\frac{\nabla_{\mathbf{r}_a}\psi(\mathbf{k}, \mathbf{r}_a)}{2\psi(\mathbf{k}, \mathbf{r}_a)}\right)\right.$$
$$\left.\times\nabla_{\mathbf{r}_b}\psi(\mathbf{k}, \mathbf{r}_b) + \frac{Z_b}{r_b}\psi(\mathbf{k}, \mathbf{r}_b)\right]\psi(\mathbf{k}, \mathbf{r}_a) = 0, \quad (4.7)$$

where β_a and β_b are the partition coefficients, $\beta_a + \beta_b = 2$.

Now suppose that each term in square brackets is equal to zero, for example,

$$\frac{1}{2}\Delta_{\mathbf{r}_a}\psi(\mathbf{k}, \mathbf{r}_a) + \left(i\mathbf{k} + \beta_a\frac{\nabla_{\mathbf{r}_b}\psi(\mathbf{k}, \mathbf{r}_b)}{2\psi(\mathbf{k}, \mathbf{r}_b)}\right)$$
$$\times\nabla_{\mathbf{r}_a}\psi(\mathbf{k}, \mathbf{r}_a) + \frac{Z_a}{r_a}\psi(\mathbf{k}, \mathbf{r}_a) = 0. \quad (4.8)$$

and consider the consequences that follow from such an assumption.

Suppose that the "two-storied" construction in parentheses is small for some reason and, hence, this ratio can be neglected. Then, the remaining equation in (4.8) possesses the analytic solution

$$\psi(\mathbf{k}, \mathbf{r}_a) = Q(\alpha_a, \mathbf{k}, \mathbf{r}_a)$$
$$\equiv {}_1F_1(i\alpha_a, 1, -i(kr_a + \mathbf{k}\mathbf{r}_a)), \quad (4.9)$$

where $\alpha_a = -Z_a/k$ is the Sommerfeld parameter. Here the wave function $\Psi(\mathbf{k}, \mathbf{r})$ takes the form

$$\Psi(\mathbf{k}, \mathbf{r}) = \exp(i\mathbf{k}\mathbf{r})\prod_{l=a}^{b} N(\alpha_l)Q(\alpha_l, \mathbf{k}, \mathbf{r}_l),$$
$$N(\alpha_l) = \exp\left(-\frac{\pi\alpha_l}{2}\right)\Gamma(1 - i\alpha_l), \quad (4.10)$$

and satisfies both the normalization condition [86]

$$\langle\Psi(\mathbf{k})|\Psi(\mathbf{k}')\rangle = \int d\mathbf{r}\Psi^*(\mathbf{k}, \mathbf{r})\Psi(\mathbf{k}', \mathbf{r})$$
$$= (2\pi)^3\delta(\mathbf{k} - \mathbf{k}') \quad (4.11)$$

and Redmond asymptotic condition

$$\lim_{kr\to\infty}\Psi(\mathbf{k}, \mathbf{r}) \longrightarrow \exp(i\mathbf{k}\mathbf{r})$$
$$\times\exp(-i(\alpha_a + \alpha_b)\ln(kr + \mathbf{k}\mathbf{r})). \quad (4.12)$$

The function in (4.10) is called the 2C wave function (or TCC, two-center Coulomb) [82]. At large values of kr, it satisfies Eq. (4.8) to an accuracy of $O((kr)^{-2})$, which is easily verifiable by substitution. It should be noted that the obtained function has the expected physical asymptotics (4.12), because a particle incident at a large impact parameter "sees" a one-center molecule. The function in (4.10) is a product of distorted waves and, thus, multiple electron rescattering on each center is taken into account.

Next, consider Eq. (4.8) in which $\nabla_{\mathbf{r}_b}\psi(\mathbf{k}, \mathbf{r}_b)/\psi(\mathbf{k}, \mathbf{r}_b)$ is replaced by its asymptotic expression,

$$\frac{\nabla_{\mathbf{r}_b}\psi(\mathbf{k}, \mathbf{r}_b)}{\psi(\mathbf{k}, \mathbf{r}_b)} \approx \alpha_b\frac{k(\mathbf{r}_b/r_b) + \mathbf{k}}{i(kr_b + \mathbf{k}\mathbf{r}_b)}q(\mathbf{k}, \mathbf{r}_b)$$
$$+ O((kr_b)^{-2}). \quad (4.13)$$

where

$$q(\mathbf{k}, \mathbf{r}_b) = 1 - \exp(-i(kr + \mathbf{k}\mathbf{r}_b))\frac{f^*(\mathbf{k}, \mathbf{r}_b)}{f(\mathbf{k}, \mathbf{r}_b)},$$
$$f(\mathbf{k}, \mathbf{r}_b) = \frac{\exp(-i\alpha_b\ln(kr_b + \mathbf{k}\mathbf{r}_b))}{\Gamma(1 - i\alpha_b)}.$$

Substitute (4.13) into (4.8); replace in it the quantity $\alpha_b\beta_b q(\mathbf{k}, \mathbf{r}_b)$ with some constant ε_a; and, considering it as a small variable parameter to be further deter-

mined with the help of a suitable criterion. We write this equation with an accuracy of $O(r_a^{-2})$:

$$\frac{1}{2}\Delta_{\mathbf{r}_a}\psi(\mathbf{k},\mathbf{r}_a)+\left(i\mathbf{k}+\frac{i\varepsilon_a}{2}\frac{k\hat{\mathbf{r}}_a+\mathbf{k}}{kr_a+\hat{\mathbf{k}}\mathbf{r}_a}\right)\nabla_{\mathbf{r}_a}\psi(\mathbf{k},\mathbf{r}_a) + \frac{Z_a}{r_a}\psi(\mathbf{k},\mathbf{r}_a) = 0, \tag{4.14}$$

where the vector $\mathbf{r}_b$ in parentheses is substituted for $\mathbf{r}_a$, since $r_b^{-1} = r_a^{-1} + O(r_a^{-2})$. The equation obtained in this way has an exact solution that depends on the parameter ε_a,

$$\psi(\mathbf{k},\mathbf{r}_a) = Q(\alpha_a,\varepsilon_a,\mathbf{k},\mathbf{r}_a) \equiv {}_1F_1(i\alpha_a, 1-i\varepsilon_a, -i(kr_a+\mathbf{k}\mathbf{r}_a)), \tag{4.15}$$

and coincides with (4.9) for $\varepsilon_a = 0$. By using (4.15) we obtain the expression for a new wave function called a modified two-center Coulomb function (MTCC),

$$\Psi(\mathbf{k},\mathbf{r}) = \exp(i\mathbf{k}\mathbf{r})\prod_{l=a}^{b}N(\alpha_l,\varepsilon_l)Q(\alpha_l,\varepsilon_l,\mathbf{k},\mathbf{r}_l), \tag{4.16}$$

where the normalization factor

$$N(\alpha,\varepsilon) = \exp(-\pi\alpha/2)\frac{\Gamma(1-i\alpha-i\varepsilon)}{\Gamma(1-i\varepsilon)}.$$

The main difference between functions (4.10) and (4.16) is that in the latter the electron relative motion in the field of one of the Coulomb centers depends on the Sommerfeld parameter of the other. This function was first obtained and used in [87].

The case of $Z_a = Z_b = Z$ is considered to be the most important from the standpoint of physics . It requires that the function in (4.16) be symmetrically represented. Let us write it in the following form ($\alpha_a = \alpha_b = \alpha$):

$$\chi(\mathbf{k},\mathbf{r}) = \frac{1}{2}\exp(i\mathbf{k}\mathbf{r})N(\alpha,\varepsilon_a)N(\alpha,\varepsilon_b) \times [Q(\alpha,\varepsilon_a,\mathbf{k},\mathbf{r}_a)Q(\alpha,\varepsilon_b,\mathbf{k},\mathbf{r}_b) + Q(\alpha,\varepsilon_a,\mathbf{k},\mathbf{r}_b)Q(\alpha,\varepsilon_b,\mathbf{k},\mathbf{r}_a)]. \tag{4.17}$$

If one assumes $\varepsilon_a = \varepsilon_b$, then Eq. (4.17) becomes identical with Eq. (4.16).

4.3. Single Ionization of Positively Charged Ion of the Hydrogen Molecule by a Fast Electron

We refer those interested in refreshing their knowledge in the field of quantum chemistry (adiabatic approximation, MOLCAO construction and their notation, molecular symmetries, etc.) to the remarkable book by Gribov [88] and review [89]. Here we shall be using conventional terminology without further references.

The simplest wave function $\Phi_{^2\Sigma_g^+}(\mathbf{r})$ that describes the ground state $^2\Sigma_g^+$ of a H_2^+ ion is obtained in the framework of the MOLCAO method by varying two parameters, f and g [82]:

$$\Phi_{^2\Sigma_g^+}(\mathbf{r}) = N(\exp(-fr_a-gr_b) + \exp(-gr_a-fr_b)), \tag{4.18}$$

where $f = 0.224086$ and $g = 1.13603$ are the variational parameters and $N(\rho) = 0.6217$ is the normalization constant. The ion binding energy is $I_1 = 30$ eV, while the equilibrium internuclear distance is $\rho = 2$.

The interaction potential between target and incident electron is chosen as follows:

$$V(\mathbf{R},\mathbf{r};\boldsymbol{\rho}) = -\frac{1}{R_a}-\frac{1}{R_b}+\frac{1}{|\mathbf{R}-\mathbf{r}|} \tag{4.19}$$

and the desired matrix element is written as

$$T_{fi}(\boldsymbol{\rho}) = \langle \mathbf{p}_s, \chi(\mathbf{k})|V(\boldsymbol{\rho})|\mathbf{p}_i, \Phi_{^2\Sigma_g^+}\rangle = \frac{4\pi}{Q^2}\int d\mathbf{r}\chi^*(\mathbf{k};\mathbf{r})[e^{i\mathbf{Q}\mathbf{r}} - e^{i\mathbf{Q}\boldsymbol{\rho}/2} - e^{-i\mathbf{Q}\boldsymbol{\rho}/2}]\Phi_{^2\Sigma_g^+}(\mathbf{r}). \tag{4.20}$$

In this representation a fast incident electron is described by the plane wave, although it could be expressed in terms of the Coulomb wave, because of the positive charge of the ion. In addition, in the framework of FBA, it is possible to carry out formal orthogonalization of the initial and final states of the target with the result that Eq. (4.20) transforms to

$$T_{fi}(\boldsymbol{\rho}) = \frac{4\pi}{Q^2}\int d\mathbf{r}\chi^*(\mathbf{k};\mathbf{r}) \times [e^{i\mathbf{Q}\mathbf{r}} - F(\mathbf{Q},\boldsymbol{\rho})]\Phi_{^2\Sigma_g^+}(\mathbf{r}), \tag{4.21}$$

where $F(\mathbf{Q},\boldsymbol{\rho}) = \langle \Phi_{^2\Sigma_g^+}|e^{i\mathbf{Q}\mathbf{r}}|\Phi_{^2\Sigma_g^+}\rangle$ is the molecular form factor.

As we are not going much into the details of calculation, the only point to be mentioned here is that one cannot avoid numerical integration. These details can be found in dissertation [90] referred to earlier in the text. The case of equal charges $Z_a = Z_b = 1$ and energy values $E_i = 2$ keV and $E_k = 50$ eV [82–84] is considered. At such an initial energy it is reasonable, to some extent, to neglect exchange between scattered and emitted electrons in the cross section, describe a fast electron by the plane wave, and assume protons be "frozen" during the ionization process. The latter leads to ρ fixed in the final state by its value in a molecule's ion.

Consider first TDCS in the two cases of orientation axis of a molecule's ion: $\varphi_\rho = 0°$, $\theta_\rho = 0°$, and $\varphi_\rho = 0°$, $\theta_\rho = 90°$. At the same time, define the parameters $\varepsilon_a = -Z_3/k$ and $\varepsilon_b = -Z_4/k$ by analogy to α, but with some effective charges Z_3, Z_4, and take them to be equal to each other for general reasons. In order to fix the opti-

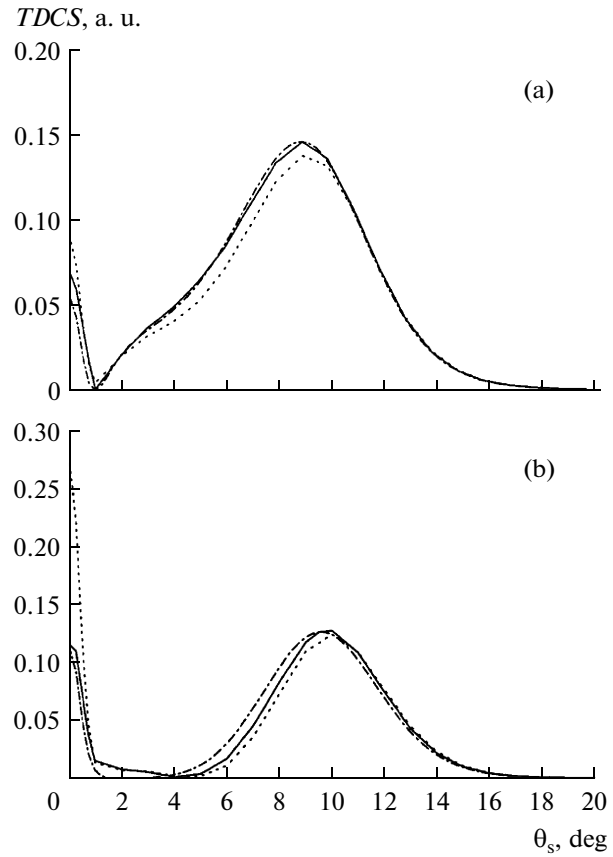

Fig. 13. Triple differential cross sections of the reaction (e,2e) on H_2^+ ion as a function of the electron scattering angle θ_s with optimal values $Z_3 = Z_4$ obtained by normalizing to the maximum at $\mathbf{k} \parallel \mathbf{Q}$ (solid curve), $Z_3 = Z_4 = 0$ (dotted curve), and [84] (dash–dotted curve): (a) $\varphi_\rho = 0°$, $\theta_\rho = 0°$; (b) $\varphi_\rho = 0°$, $\theta_\rho = 90°$. The figure is taken from [87].

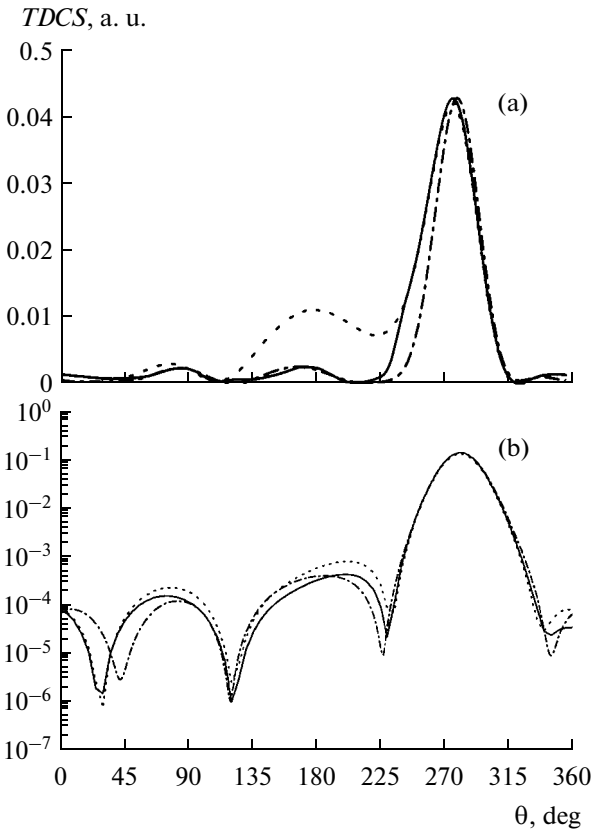

Fig. 14. Triple differential cross sections of the reaction (e,2e) as a function of the electron emission angle θ with values $Z_3 = Z_4$ obtained by normalizing to the principal peak (solid curve), $Z_3 = Z_4 = 0$ (dotted curve), and [84] (dash–dotted curve). Here $\varphi_\rho = 0°$, $\theta_\rho = 0°$, $\theta_s = 3°$ (a), $\theta_s = 9°$ (b). The figure is taken from [87].

mal value $Z_3 = Z_4$, comparison of maxima of results for the cross section calculations according to (4.21) and those obtained by numerical computations in the prolate spheroid coordinates [84] was carried out. This maximum is reached in the case of the momentum of emitted electron is equal and parallel to the momentum transfer, i.e., $\mathbf{k} = \mathbf{Q}$. This is the so-called "Bethe ridge," when the recoil momentum $\mathbf{K} = 0$ and the absolute maximum of the cross section is observed. The required equality $Z_3 = Z_4$ was defined by the minimal value in the difference of the cross sections in the vicinity of this maximum. As a consequence of applying such a "variational principle," it was found that $Z_3 = Z_4$ does not exceed 0.2. It was also noted that the function $Z_3 = Z_4 = f(\theta_s)$ depends weakly on both the scattering and molecule orientation $\theta\rho$ angles.

In Figs. 13a and 13b, the TDCSs are shown as functions of the electron scattering angle for $\mathbf{k} \parallel \mathbf{Q}$ in the case of two orientations of the molecule's axis: $\varphi_\rho = 0°$, $\theta_\rho = 0°$ and $\varphi_\rho = 0°$, $\theta_\rho = 90°$. In the case of $\mathbf{k} \parallel \mathbf{Q}$, the recoil momentum reaches its minimum and the maximal collision energy is transferred to emitted electron. From Fig. 13 it is seen that the introduction of additional parameter ε slightly improves the agreement with results [84], especially in the region of small scattering angles, where the two-center model proposed in [82] barely works.

In order for the effects of Z_3 and Z_4 parameter introduction to be seen in a greater detail, consider the TDCS in its dependence on the electron scattering angle for two directions of scattered electron $\theta_s = 3°$ (Fig. 14a) and $\theta_s = 9°$ (Fig. 14b) and the molecule's axis orientation $\varphi_\rho = 0°$, $\theta_\rho = 0°$. Improvement of the approximate wave function upon introduction of additional parameters ε_l is evident from Figs. 14a and 14b in the range $100° < \theta < 240°$. Some discrepancies still persist in the range $0° < \theta < 100°$ (seen in Fig. 14b), which are hard to interpret, since here the differential cross section drops by more than three orders of magnitude with respect to the absolute maximum; this discrepancy can be attributed to a certain roughness of approximation of the wave function (4.16).

4.4. Single Ionization of the Hydrogen Molecule by the Electron Impact

Now consider a single ionization of the hydrogen molecule by the electron impact,

$$e + H_2(^2\Sigma_g^+) \longrightarrow 2e + H_2^+(^2\Sigma_g^+).$$

The triple differential cross section $\sigma^{(3)}$ is calculated according to formula (4.4.1), the potential of a molecule single ionization $I = 16$ eV, its equilibrium internuclear distance $\rho = 1.4354$ au, and the amplitude T_{fi} for an unpolarized fast electron looks like

$$T_{fi} = \sqrt{2}\int \mathbf{dR}\int \mathbf{dr}_1\int \mathbf{dr}_2 \exp(i\mathbf{QR})\chi^*(\mathbf{k}_1;\mathbf{r}_1) \times \Phi_{^2\Sigma_g^+}(\mathbf{r}_2) V \Phi_{^1\Sigma_g^+}(\mathbf{r}_1, \mathbf{r}_2). \quad (4.22)$$

The potential V defines an interaction of incident electron with target H_2 for the following values of nuclear charges $Z_a = Z_b = 1$:

$$V = -\frac{Z_a}{R_a} - \frac{Z_b}{R_b} + \frac{1}{r_{1p}} + \frac{1}{r_{2p}}. \quad (4.23)$$

The wave functions $\Phi_{^1\Sigma_g^+}(\mathbf{r}_1, \mathbf{r}_2)$ and $\Phi_{^2\Sigma_g^+}(\mathbf{r}_2)$ that describe ground states $^1\Sigma_g^+$ and $^2\Sigma_g^+$ of the molecule H_2 and molecular ion H_2^+ were taken from variational calculation [91]:

$$\Phi_{^1\Sigma_g^+}(\mathbf{r}_1, \mathbf{r}_2) = N_i \varphi(1)\varphi(2), \quad (4.24.1)$$

$$\varphi(j) = \exp(-\beta_1 r_{ja} - \beta_2 r_{jb}) + \exp(-\beta_2 r_{ja} - \beta_1 r_{jb}),$$
$$\Phi_{^2\Sigma_g^+}(\mathbf{r}_2) = N_f(\exp(-\alpha r_{2a}) + \exp(-\alpha r_{2b})), \quad (4.24.2)$$

where $\beta_1 = 0.07112$, $\beta_2 = 1.12023$, $\alpha = 1.23$, $N_i = 0.169937$, and $N_f = 0.423547$. The wave function $\chi(\mathbf{k}_1; \mathbf{r}_{1a}, \mathbf{r}_{1b})$, describing the state that belongs to the continuous spectrum of a slow emitted electron, is determined by formula (4.17).

The triple differential cross sections of the ionization process of helium atom and hydrogen molecule calculated for $E_s = 500$ eV; $E_1 = 37$, 74, and 205 eV; and $\theta_s = 6°$ are shown in Fig. 15. Theoretical evaluations are done for helium atom by using one of the variations of the convergent close coupling (CCC) method [93], while, for a hydrogen molecule, they are done—in the FBA and distorted wave (M3DW, molecular three-body distorted wave) approximations with averaging over orientations of the molecule's axis [94, 95]. In FBA approximations the fitting parameter $Z_3 = Z_4$ was fixed by normalization of binary maximum to the experiment.

Let us start with analyzing the results for a helium atom presented in Figs. 15a–15c. Good agreement between experiment and theory is observed in both the shape of the distribution as a whole and the positions of binary peaks. At the same time, a more detailed comparison reveals a shift in binary peak by no more than 10° away from the direction of the momentum transfer θ_Q. This feature is well known from the studies of a single ionization of a helium atom [12, 96] and reflects the insufficiency of the FBA approximation, when the energies of emitted and scattered electrons become comparable.

In the case of a hydrogen molecule (Figs. 15d–15f), comparison of experiment and theory gives a less satisfactory result. A certain agreement between the FBA and M3DW calculations is observed at low energies of an emitted electron (Fig. 15d–15e), whereas the M3DW model describes better the vicinity of the binary peak at high energies (Fig. 15f). Note that the M3DW model predicts the existence of a shoulder in the binary peak (Fig. 15f) at $E_1 = 205$ eV, which, however, cannot be observed due to poor statistics of the experiment.

From Fig. 15 it follows that triple differential cross sections of reactions (e,2e) for helium atom and hydrogen molecule resemble each other in shape, particularly in the region of a binary peak at low ionized electron energies. This is easily seen, since, under such conditions, the reaction takes place at a high impact parameter (a low momentum transfer) and, therefore, both protons of the molecule are felt by an incident electron as if they resided at the same point and had a charge identical to that of a helium atom nucleus. At the same time, noticeable distinctions are observed in the region of the recoil peak, i.e., in the direction opposite to that of the momentum transfer $\theta_{-Q} = \theta_Q + \pi$, as here the mechanisms related with interior of the target are important.

4.5. Double Ionization of the Hydrogen Molecule by the Electron Impact

Finally, let us direct our attention to a double ionization of the hydrogen molecule H_2 by the electron impact,

$$e + H_2 \longrightarrow 3e + H^+ + H^+.$$

The fivefold differential cross section $\sigma^{(5)}$ averaged over directions of the molecule axis is expressed by formula (4.4.2). In this case the double ionization potential $IP = 51$ eV, the distance between nuclei $\rho = 1.4354$ au, and the amplitude T_{fi} has the following form:

$$T_{fi} = \sqrt{2}\int \mathbf{dR}\int \mathbf{dr}_1\int \mathbf{dr}_2 \exp(i\mathbf{QR})\chi_f^*(\mathbf{k}_1, \mathbf{k}_2;\mathbf{r}_1, \mathbf{r}_2) \times V\Phi_{^1\Sigma_g^+}(\mathbf{r}_1, \mathbf{r}_2). \quad (4.25)$$

The potential V is the same as in (4.23).

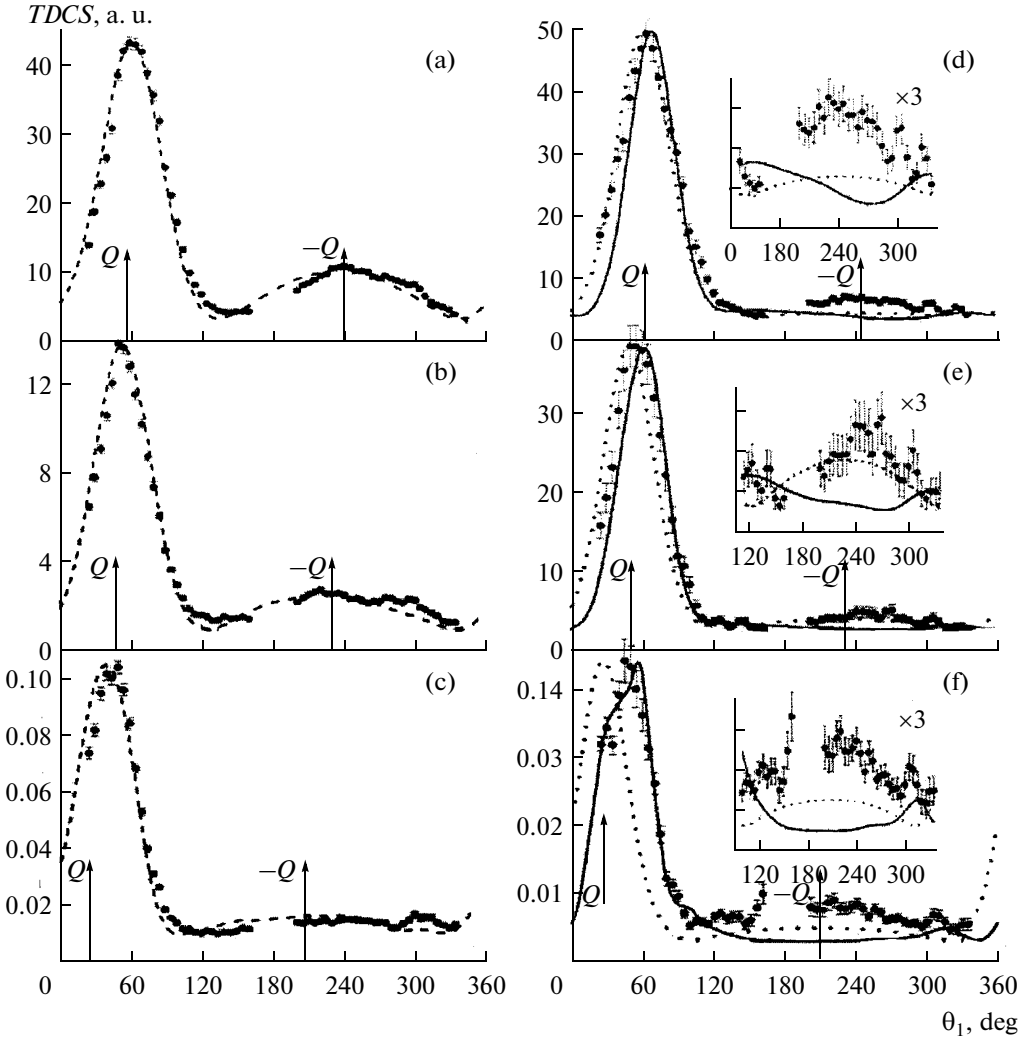

Fig. 15. Triple differential cross sections of the reaction (e,2e) on helium atom (a left panel) and H_2 molecule (a right panel) as a function of the electron emission angle θ_1 (counted clockwise). Dashed curve—CCC, dotted curve—FBA, and solid curve—M3DW. The experimental data are taken from [92] at the energies $E_1 = 37$ eV (a, d), 74 eV (b, e), and 205 eV (c, f). The figure is borrowed from [92].

The trial three-parameter wave function of the ground state of $\Phi_{^1\Sigma_g^+}(\mathbf{r}_1, \mathbf{r}_2)$ molecule somewhat differs from (4.24.1) [97]:

$$\Phi_{^1\Sigma_g^+}(\mathbf{r}_1, \mathbf{r}_2) = N(\phi(1)\psi(2) + \psi(1)\phi(2)), \quad (4.26)$$

where

$$\phi(j) = x_a(j) + \varepsilon x_b(j), \quad \psi(j) = \varepsilon x_a(j) + x_b(j),$$
$$x_a(j) = \exp(-\beta\xi_j - \gamma\eta_j),$$
$$x_b(j) = \exp(-\beta\xi_j + \gamma\eta_j),$$

$\xi_j = (r_{ja} + r_{jb})/\rho$, $\eta_j = (r_{ja} - r_{jb})/\rho$, $\beta = 0.835$, $\gamma = 0.775$, and $\varepsilon = 0.137$ are the variational parameters; and $N = 0.255$ is the normalization constant.

The final state nonsymmetrized wave function $\chi_f(\mathbf{k}_1, \mathbf{k}_2; \mathbf{r}_1, \mathbf{r}_2)$ of two slow emitted electrons in the field of two nuclei at rest is represented as the sum of a product of two MTCC (4.17) multiplied by the so-called Gamov factor,

$$\chi_f(\mathbf{k}_1, \mathbf{k}_2; \mathbf{r}_1, \mathbf{r}_2) = N(\alpha_{12})\chi(\mathbf{k}_1, \mathbf{r}_1)\chi(\mathbf{k}_2, \mathbf{r}_2),$$
$$N(\alpha_{12}) = \exp(-\pi\alpha_{12}/2)\Gamma(1 - i\alpha_{12}), \quad (4.27)$$
$$\alpha_{12} = \frac{1}{|\mathbf{k}_1 - \mathbf{k}_2|}.$$

Denote also small parameters $\varepsilon_1 = \varepsilon_{1a} = \varepsilon_{1b}$ and $\varepsilon_2 = \varepsilon_{2a} = \varepsilon_{2b}$.

It should be noted that taking into account interelectronic correlations in a separable function of the final state by means of the Gamov factor is not the best path to follow in the case of slowly moving electrons, although it is commonly used for estimates. As a rule, its introduction into the cross section calculation leads to sizable decrease of the latter, even though behavior

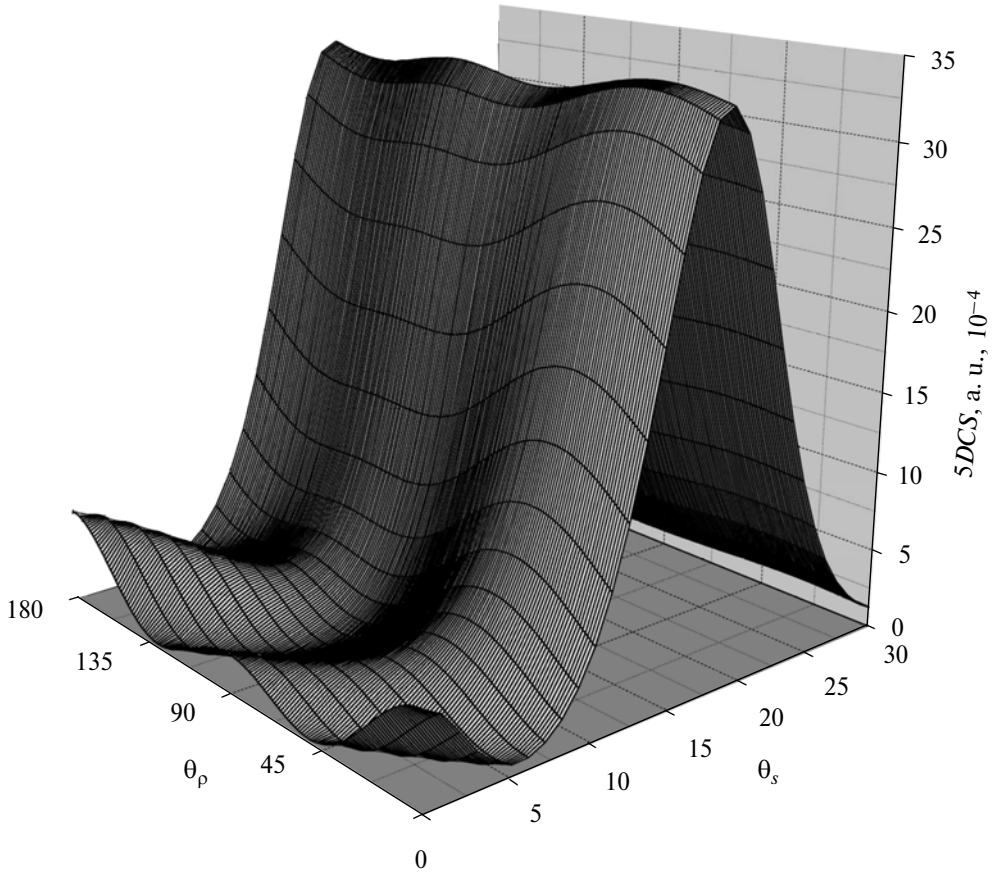

Fig. 16. Fivefold differential cross section of the reaction (e,3e) vs. electron scattering angle θ_s and molecule orientation θ_ρ at $\mathbf{k}_1 \uparrow\uparrow \mathbf{Q}$ and $\mathbf{k}_2 \downarrow\uparrow \mathbf{Q}$. Here $\varepsilon_1 = \varepsilon_2 = 0$ and $E_i = 612$ eV. The figure is taken from [100].

of the cross section is correct in terms of physics (its equality to zero) for $\mathbf{k}_1 = \mathbf{k}_2$.

Integration over the **R** coordinate of a fast incident electron is trivial, while the remaining 6D integral transforms to several 3D integrals of a product of the functions of type (3.24), which are numerically evaluated. For details refer to [90]; here we omit them altogether.

Now take the energies of incident and emitted electrons to be 612, 51, and 10 eV, respectively, as was done in [98]. The 5DCS quoted in Eq. (4.3.2) is shown in Fig. 16 as a function of electron scattering θ_s and molecule axis orientation θ_ρ angles for opposite directions of slow electrons with $\mathbf{k}_1$ being parallel to **Q**. Two peaks at $\theta_\rho = 170°$ and 80° are observed in the region of small scattering angles 0°–5°. These regions correspond to the molecule's axis oriented in parallel and perpendicular directions to that of the momentum transfer **Q**. Note that in the experiment geometry chosen, the recoil momentum **K** is parallel to **Q**, which follows from the law of conservation of momentum,

$$\mathbf{Q} = \mathbf{p}_i - \mathbf{p}_s = \mathbf{k}_1 + \mathbf{k}_2 + \mathbf{K}.$$

As the electron scattering angle increases, these two peaks are seen to follow along directions of the momentum transfer until the cross section reaches its maximum at $\theta_s = 16.5°$. One can verify that $\mathbf{Q} = \mathbf{k}_1$, i.e., for all the molecule orientations θ_ρ the condition $\mathbf{k}_2 = -\mathbf{K}$ is satisfied. As the calculations show, the 5DCS is relatively less sensitive to the variations in θ_ρ rather than θ_s. Such a situation exactly corresponds to the so-called "Bethe ridge" in (e,2e) single ionization, when the target recoil momentum is low compared to the momentum transfer and a nucleus of the molecule takes virtually no part in the reaction.

Now consider the FDCS presented in (4.4.2) and averaged over the orientations of a molecule's axis. The high (5612 eV) and medium (612 eV) values of the incident electron energy are examined for the same values of emitted electron energies of 51 and 10 eV. The FDCS is shown in Figs. 17a and 17b as a function of the first emitted electron angle θ_1, with $\theta_s = 0.45°$ ($E_i = 5612$ eV) and $\theta_s = 1.5°$ ($E_i = 612$ eV), and $\mathbf{k}_2$ parallel to **Q**. It can be noted that, in both cases, the opposite directions of emitted electron momenta ensure a maximal value of FDCS.

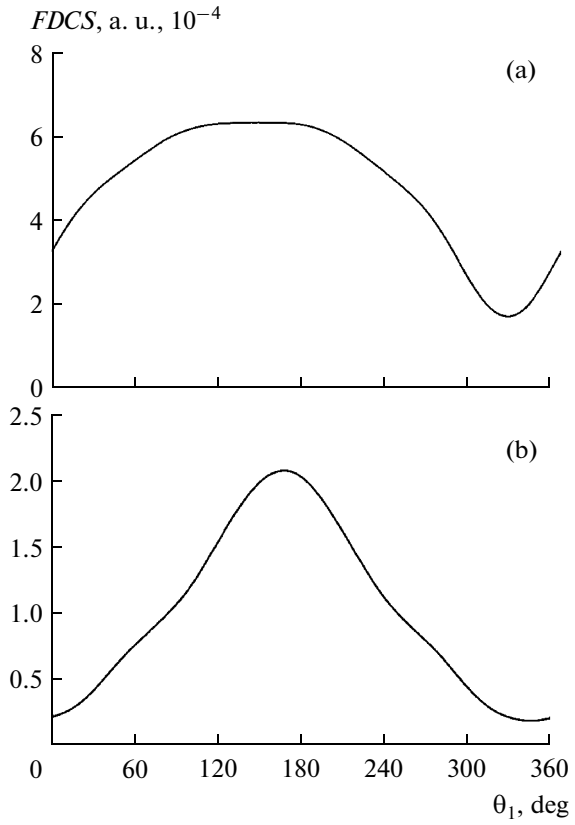

Fig. 17. Averaged fivefold differential cross sections of the reaction (e,3e) as a function of the electron emission angle θ_1 at $\mathbf{k}_2 \uparrow\uparrow \mathbf{Q}$: (a) $E_i = 5612$ eV, $\theta_s = 0.45°$, and $\theta_2 = 322°$; (b) $E_i = 612$ eV, $\theta_s = 1.5°$, and $\theta_2 = 346°$. Here $\varepsilon_1 = \varepsilon_2 = 0$. The figure is borrowed from [100].

Both these calculations are apparently qualitative, since, as we know, (e,3e) experiments with molecules, and even more so the oriented ones, were not conducted.

4.6. Discussion of Section 4 Results

In this section we have discussed the possibility for the complex four- and five-body final state wave functions of a quantum system to be simply and adequately represented, rather than the physical results of single and double ionization of the simplest hydrogen molecule (a positively charged ion H_2^+) by the electron impact. To this end, a distorted wave method was developed that described the behavior of each molecular electron in the Coulomb field of two heavy centers.

In principle, the model has two fitting parameters that can be reduced to just one parameter, much like in the effective charge model. It works well in the case of single ionization and competes not only with other approximate schemes, but also with complicated numerical computations in a wide range of angles and energies of emitted electron.

In the case of double ionization, we presented a variant that does not fully take into account ee correlations in the final state. Nevertheless, in this case the model is still satisfactory, although only qualitatively. Consider the experimental results of (e,3 − 1e) reaction with a molecular target [98]. In these experiments one explores the double ionization of a hydrogen molecule, with a scattered and only one emitted electron

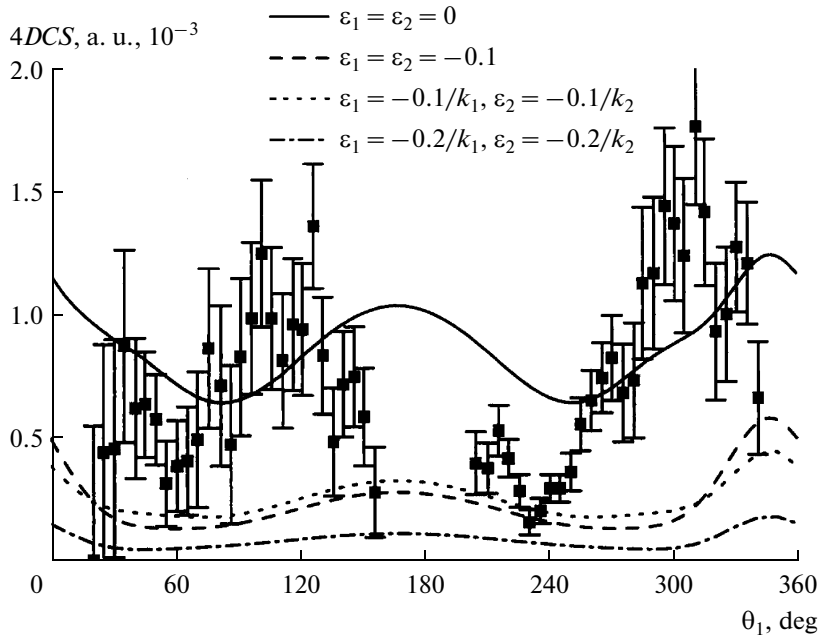

Fig. 18. Fourfold differential cross section of the reaction (e,3 − 1e) as a function of the electron emission angle θ_1 at $\theta_s = 1.5°$. The experimental data are taken from [98] and scaled to match theoretical results at $\varepsilon_1 = \varepsilon_2 = 0$ in the region close to the maximum of a binary peak (about 300°): $E_i = 612$ eV, $E_1 = 51$ eV, and $E_2 = 10$ eV. The figure is taken from [100].

detected in coincidence. From the experimental point of view, such measurements allow the signal-to-background ratio to be considerably increased, thus ensuring reliability of the results obtained. To be able to confront the experiment (on a relative scale) with the theory, it suffices to integrate the FDCS over the spherical angle Ω_2 of a second slow emitted electron,

$$\bar{\sigma}^{(4)} = \int d\Omega_2 \bar{\sigma}^{(5)}$$

and appropriately "scale" the experiment. From Fig. 18 it follows that, for any choice of ε_i, the model considered reproduces the shape of experimental distribution with two maxima and minima, which, however, are somewhat shifted with respect to the experimental ones. All the theoretical results give a dominating maximum in the cross section close to the direction of $\mathbf{Q}$ at $\theta_1 = 350°$. A certain discrepancy between the FBA theory presented in this work and the experiment is also observed in the case of single ionization, especially for medium values of the energy of an incident electron. At high energies of that electron, this discrepancy disappears [99], which points to the necessity of using SBA calculations in further studies.

CONCLUSIONS

In this review we tried to highlight just a few theoretical approaches to the problem of multiple ionization of atomic or molecular target by a fast charged particle. Such popular and powerful, from the computational point of view, theoretical concepts as the convergent close-coupling method, the *J*-matrix method, etc., were omitted. As was already noted in the Introduction, "no living man all things can." Therefore, we were guided by the idea of exposing approaches and approximations "filled" with and understandable from the physics point of view, rather than some "bare" numerical schemes that allow achieving good agreement with experiment. Surely enough, in such a way it is impossible to give a complete picture of the considered physical models. Rather, our goal was primarily to highlight the essence of these models and show their practical capabilities.

The multiple ionization experiments with measurements of energies and emission angles of the final fragments in coincidence are very informative and, at the same time, quite complicated. Nonetheless, there has been considerable progress in this direction in recent decades: new kinematical regions are becoming accessible for investigation that were once thought to be virtually inaccessible. This, in turn, requires going beyond the usual approximations (such as, e.g., the FBA).

It should be noted that atomic processes have recently drawn the attention of both theorists and experimenters in high energy physics, a field seemingly too removed in energy from that considered here (see, for example, review [101] devoted to atomic physics experiments on cyclic and linear accelerators). It should also be mentioned that it appears possible to study the processes of quantum target multiple ionization by a charged particle in the presence of an intense laser field. Eventually, experimental development poses new challenges for the theory.

ACKNOWLEDGMENTS

This work has been carried out within the JINR topical plan 09-6-1060-2005/2010 "Mathematical Support of Experimental and Theoretical Studies Conducted by JINR" and the Russian Foundation for Basic Research (project no. 08-01-00604-a, "Mathematical Simulation of the Dynamics of Light Atoms and Molecules Due to Interactions with Fast Particles, Laser Pulses, and Magnetic Fields"). The authors are grateful to S.I. Vinitsky, V.V. Serov, and B. Joulakian for their helpful comments and stimulating discussions.

REFERENCES

1. L. D. Faddeev, *Mathematical Problems of the Quantum Theory of Scattering for a Three-Particle System*, Tr. MIAN SSSR (1963), vol. 69.
2. L. D. Faddeev and S. P. Merkuriev, *Quantum Scattering Theory for Several Particle Systems* (Kluwer, Dordrecht, 1993) [in Russian].
3. S. P. Merkuriev, Teor. Mat. Fiz. **32**, 187 (1977); S. P. Merkuriev, Acta Phys. Austr. **23** (Suppl.), 65 (1981).
4. V. L. Shablov, P. S. Vinitsky, Yu. V. Popov, O. Chuluunbaatar, and K. A. Kouzakov, Fiz. Elem. Chastits At. Yadra **41** (2) 607 (2010) [Phys. Part. Nucl. 41, 334 (2010)].
5. A. Kheifets, I. Bray, A. Lahmam-Bennani, A. Duguet, and I. Taouil, J. Phys. B: At. Mol. Opt. Phys. **32**, 5047 (1999).
6. A. Lahmam-Bennani, I. Taouil, A. Duguet, M. Lecas, L. Avaldi, and J. Berakdar, Phys. Rev. A **59**, 3548 (1999).
7. V. G. Neudachin, Yu. V. Popov, and Yu. F. Smirnov, Usp. Fiz. Nauk **169**, 1111 (1999) [Phys. Usp. **42**, 1017 (1999)].
8. N. Watanabe, Y. Khajuria, M. Takahashi, Y. Udagawa, P. S. Vinitsky, Yu. V. Popov, O. Chuluunbaatar, and K. A. Kouzakov, Phys. Rev. A **72**, 032705 (2005).
9. R. K. Peterkop, Opt. Spektrosk. **13**, 153 (1962).
10. R. K. Peterkop, *Theory of Ionisation of Atoms* (Zinatne, Riga, 1975; Colorado Assoc. Univ., 1977).
11. M. R. H. Rudge and M. J. Seaton, Proc. R. Soc. London Ser. A **283**, 262 (1965).
12. A. Lahmam-Bennani, J. Phys. B: At. Mol. Opt. Phys. **24**, 2401 (1991).
13. J. Berakdar, A. Lahmam-Bennani, and C. Dal Cappello, Phys. Rep. **374**, 91 (2003).
14. E. Weigold and I. E. McCarthy, *Electron Momentum Spectroscopy* (Kluwer, New York, 1999).
15. M. A. Coplan, J. H. Moore, and J. P. Doering, Rev. Mod. Phys. **66**, 985 (1994).
16. J. S. Briggs and M. Schmidt, J. Phys. B: At. Mod. Opt. Phys. **33**, R1 (2000).

17. H. R. Sadeghpour, Can. J. Phys. **74**, 727 (1996).
18. P. Lambropoulus, P. Maragakis, and J. Zhang, Phys. Rep. **305**, 203 (1998).
19. V. M. Lend'el, V. Yu. Lazur, M. M. Karbovanets, and R. K. Yanev, *Introduction to the Theory of Atomic Collisions* (Vyshcha Shkola, Lvov, 1989) [in Russian].
20. Dž. Belkić, R. Gayet, and A. Salin, Phys. Rep. **56**, 279 (1979).
21. Dž. Belkić, I. Mančev, and J. Hanssen, Rev. Mod. Phys. **80**, 249 (2008).
22. M. Inokuti, Rev. Mod. Phys. **43**, 297 (1971).
23. J. D. Dollard, J. Math. Phys. **5**, 729 (1964).
24. V. V. Komarov, A. M. Popova, and V. L. Shablov, *Few Quantum Particle System Dynamics* (Mosc. Univ., Moscow, 1996) [in Russian].
25. V. L. Shablov, V. A. Bilyk, and Yu. V. Popov, Fundam. Prikl. Matem. **4**, 1207 (1998).
26. V. L. Shablov, V. A. Bilyk, and Yu. V. Popov, in *Many-Particle Spectroscopy of Atoms, Molecules, Clusters, and Surfaces*, Ed. by J. Berakdar and J. Kirshner (Kluwer Acad., Plenum, New York, 2001), p. 71.
27. H. Erhardt, G. Knoth, P. Schlemmer, and K. Jung, Phys. Lett. A **110**, 92 (1885).
28. P. Schlemmer, T. Rösel, K. Jung, and H. Erhardt, Phys. Rev. Lett. **63**, 252 (1989).
29. Yu. V. Popov, C. Dal Cappello, and K. Kouzakov, J. Phys. B: At. Mol. Opt. Phys. **29**, 5901 (1996).
30. E. A. Hylleraas, Zeit. Physik. A **54**, 347 (1929).
31. E. Clementi and C. Roetti, At. Nucl. Data, Data Tables **14**, 177 (1974).
32. C. Eckart, Phys. Rev. **36**, 878 (1930).
33. S. Chandrasekhar, Astrophys. J. **100**, 176 (1944).
34. O. Chuluunbaatar, I. V. Puzynin, and S. I. Vitinsky, J. Phys. B: At. Mol. Opt. Phys. **34**, L425 (2001).
35. J. Mitroy, I. E. McCarthy, and E. Weigold, J. Phys. B: At. Mol. Opt. Phys. **18**, 4149 (1985).
36. R. A. Bohnam and D. A. Kohl, J. Chem. Phys. **45**, 2471 (1966).
37. S. T. Hood, I. E. McCarthy, P. J. O. Teubner, and E. Weigold, Phys. Rev. A **8**, 2494 (1973).
38. K. T. Leung, in *Theoretical Models of Chemical Bonding*, Pt. 3, Ed. by Z. B. Maksic (Springer, Berlin, 1991).
39. N. Lermer, B. R. Todd, N. M. Cann, C. E. Brion, Y. Zheng, S. Chakravorty, and E. R. Davidson, Can. J. Phys. **74**, 748 (1996).
40. N. Watanabe, K. A. Kouzakov, Yu. V. Popov, and M. Takahashi, Phys. Rev. A **77**, 032725 (2008).
41. R. Tweed, Z. Phys. D **23**, 309 (1992).
42. Yu. V. Popov, O. Chuluunbaatar, S. I. Vinitsky, L. U. Ancarani, C. Dal Cappello, and P. S. Vinitsky, Zh. Eksp. Teor. Fiz. **122**, 717 (2002) [JETP **95**, 620 (2002)].
43. N. V. Novikov and Ya. A. Teplova, "Charge-Changing Cross Sections in Ion-Atom Collisions," http://cdfe.sinp.msu.ru/services/cccs/cccs.htm.
44. T. A. Carlson and M. A. Krause, Phys. Rev. **140**, 1057 (1965).
45. V. Mergel, R. Dörner, Kh. Khayyat, M. Achler, et al., Phys. Rev. Lett. **86**, 2257 (2001).
46. H. Schmidt-Böcking, V. Mergel, L. Schmidt, R. Dörner, et al., Rad. Phys. Chem. **68**, 41 (2003).
47. H. Schmidt-Böckking, V. Mergel, R. Dörner, H. J. Lüdde, et al., in *Many-Particle Quantum Dynamics in Atomic and Molecular Fragmentation*, Ed. by J. Ullrich and V. P. Shevelko (Springer, 2003).
48. M. Schöffler, A. L. Godunov, C. T. Whelan, H. R. J. Walters, et al., J. Phys. B: At. Mol. Opt. Phys. **38**, L123 (2005).
49. S. Houamer, Yu. V. Popov, C. Dal Cappello, and C. Champion, Nucl. Instrum. Methods Phys. Res. B **267**, 802 (2009).
50. R. K. Nesbet and R. E. Watson, Phys. Rev. **110**, 1073 (1958).
51. S. Houamer, Yu. V. Popov, and C. Dal Cappello, Phys. Rev. A **81**, 032703 (2010).
52. A. L. Godunov, J. H. McGuire, V. S. Schipakov, H. R. J. Walters, and C. T. Whelan, Phys. B: At. Mol. Opt. Phys. **39**, 987 (2006).
53. J. Pàalinkàs, R. Schuch, H. Cederquist, and O. Gustafsson, Phys. Rev. Lett. **63**, 2464 (1989).
54. S. Alston, Phys. Rev. A **42**, 331 (1990).
55. R. R. Lewis, Jr., Phys. Rev. **102**, 537 (1956).
56. M. Brauner, J. S. Briggs, and H. Klar, J. Phys. B: At. Mol. Opt. Phys. **22**, 2265 (1989).
57. B. Joulakian and C. Dal Cappello, Phys. Rev. A **47**, 3788 (1993).
58. A. Lahmam-Bennani, I. Taouil, A. Duguet, M. Lecas, L. Avaldi, and J. Berakdar, Phys. Rev. A **59**, 3548 (1999).
59. M. A. Kornberg and J. E. Miraglia, Phys. Rev. A **48**, 3714 (1993).
60. T. Kato, Commun. Pure Appl. Math. **10**, 151 (1957).
61. O. Chuluunbaatar, I. V. Puzynin, P. S. Vinitsky, Yu. V. Popov, K. A. Kouzakov, and C. Dal Cappello, Phys. Rev. A **74**, 014703 (2006).
62. C. Le Sech, J. Phys. B: At. Mol. Opt. Phys. **30**, L47 (1997).
63. L. U. Ancarani, T. Montagnese, and C. Dal Cappello, Phys. Rev. A **70**, 012711 (2004).
64. N. Bohr, Phil. Mag. **25**, 10 (1913); Phil. Mag. **30**, 581 (1915).
65. H. Bethe, Ann. Phys. **5**, 325 (1930); Z. Phys. **76**, 293 (1932).
66. U. Fano, Phys. Rev. **95**, 1198 (1954).
67. D. P. Almeida, A. C. Fontes, and C. F. L. Godinho, J. Phys. B: At. Mol. Opt. Phys. **28**, 3335 (1995).
68. J. Lecointre, J. J. Jureta, and P. Defrance, J. Phys. B: At. Mol. Opt. Phys. **41**, 095204 (2008).
69. J. H. McGuire, M. B. Hidalgo, G. D. Doolen, and J. Nutall, Phys. Rev. A **7**, 973 (1973).
70. A. C. Roy, A. K. Das, and N. C. Sil, Phys. Rev. A **23**, 1662 (1981).
71. V. A. Sidorovich, J. Phys. B: At. Mol. Opt. Phys. **14**, 4805 (1981).
72. P. Defrance, J. J. Jureta, T. Kereselidze, J. Lecointre, and Z. S. Machavariani, J. Phys. B: At. Mol. Opt. Phys. **42**, 025202 (1981).
73. A. W. Malcherek and J. S. Briggs, J. Phys. B: At. Mol. Opt. Phys. **30**, 4419 (1997); A. W. Malcherek,

J. M. Rost, and J. S. Briggs, Phys. Rev. A **55**, R3979 (1997).

74. J. Berakdar, Phys. Lett. A **220**, 237 (1996); Phys. Lett. A **277**, 35 (2000); Phys. Rev. A **55**, 1994 (1997).
75. J. Berakdar, Phys. Rev. A **54**, 1480 (1996).
76. S. A. Zaytsev, J. Phys. A: Math. Theor. **41**, 265204 (2008).
77. S. A. Zaytsev, J. Phys. A: Math. Theor. **42**, 015202 (2009).
78. Y. D. Wang, J. H. McGuire, and R. D. Rivarola, Phys. Rev. A **40**, 3673 (1989).
79. S. E. Corchs, R. D. Rivarola, J. H. McGuire, and Y. D. Wang, Phys. Rev. A **47**, 201 (1993).
80. S. E. Corchs, R. D. Rivarola, J. H. McGuire, and Y. D. Wang, Physica Scr. **50**, 469 (1994).
81. M. Takahashi, N. Watanabe, Y. Khajuria, K. Nakayama, Y. Udagawa, and J. H. D. Eland, J. Electron Spectrosc. Relat. Phenom. **141**, 83 (2004).
82. B. Joulakian, J. Hanssen, R. Rivarola, and A. Motassim, Phys. Rev. A **54**, 1473 (1996).
83. V. V. Serov, V. L. Derbov, B. B. Joulakian, and S. I. Vinitsky, Phys. Rev. A **63**, 062711 (2001).
84. V. V. Serov, B. B. Joulakian, D. V. Pavlov, I. V. Puzynin, and S. I. Vinitsky, Phys. Rev. A **65**, 062708 (2002).
85. V. V. Serov and B. B. Joulakian, Phys. Rev. A **80**, 062713 (2009).
86. P. F. R. Weck, PhD Thesis (Univ. Metz, France, 2001).
87. O. Chuluunbaatar, B. B. Joulakian, Kh. Tsookhuu, and S. I. Vinitsky, J. Phys. B: At. Mol. Opt. Phys. **37**, 2607 (2004).
88. L. A. Gribov, *Introduction to Molecular Spectroscopy* (Nauka, Moscow, 1976) [in Russian].
89. G. Chen, S. A. Chin, Yu. Dou, et al., Adv. At. Mol. Opt. Phys. **51**, 93 (2005).
90. O. Chuluunbaatar, Doctoral Dissertation in Mathematical Physics (Dubna, JINR, Lab. Inform. Tekhnol., 2010).
91. F. Berencz, Acta Phys. Acad. Sc. Hung. **6**, 423 (1957).
92. E. M. Staicu Casagrande, A. Naja, F. Mezdari, A. Lahmam-Bennani, et al., J. Phys. B: At. Mol. Opt. Phys. **41**, 025204 (2008).
93. I. Bray, D. V. Fursa, A. Kheifets, and A. T. Stelbovics, J. Phys. B: At. Mol. Opt. Phys. **35**, R117 (2002).
94. J. F. Gao, D. H. Madison, and J. L. Peacher, Phys. Rev. A **72**, 020701 (2005).
95. J. F. Gao, D. H. Madison, and J. L. Peacher, J. Chem. Phys. **123**, 204314 (2005).
96. H. Ehrhardt, K. Jung, G. Knoth, and P. Schlemmer, Z. Phys. D **1**, 3 (1986).
97. C. Mueller and H. Eyring, J. Chem. Phys. **19**, 1495 (1951).
98. A. Lahmam-Bennani, A. Duguet, and S. Roussin, J. Phys. B: At. Mol. Opt. Phys. **35**, L59 (2002).
99. P. F. Weck, O. A. Fojón, B. Joulakian, C. R. Stia, J. Hanssen, and R. D. Rivarola, Phys. Rev. A **66**, 012711 (2002).
100. O. Chuluunbaatar, B. B. Joulakian, I. V. Puzynin, Kh. Tsookhuu, and S. I. Vinitsky, J. Phys. B: At. Mol. Opt. Phys. **41**, 015204 (2008).
101. A. S. Artemov, Fiz. Elem. Chastits At. Yadra **39**, 735 (2008) [Phys. Part. Nucl. **39**, 382 (2008)].